Safety Regulation Group

Civil Aviation Authority

CAA PAPER 2003/7

Effect of Helicopter Rotors on GPS Reception

www.caa.co.uk

Safety Regulation Group

Civil Aviation Authority

CAA PAPER 2003/7

Effect of Helicopter Rotors on GPS Reception

December 2003

ISBN 0 86039 946 X

Issued December 2003

Enquiries regarding the content of this publication should be addressed to:
Research Management Department , Safety Regulation Group, Civil Aviation Authority, Aviation House, Gatwick Airport South, West Sussex, RH6 0YR.

The latest version of this document is available in electronic format at www.caa.co.uk, where you may also register for e-mail notification of amendments.

Printed copies and amendment services are available from: Documedia Solutions Ltd., 37 Windsor Street, Cheltenham, Glos., GL52 2DG.

List of Effective Pages

Page	Date
iii	December 2003
iv	December 2003
v	December 2003
1	December 2003
2	December 2003
3	December 2003
4	December 2003
5	December 2003
6	December 2003
7	December 2003
8	December 2003
9	December 2003
10	December 2003
11	December 2003
12	December 2003
13	December 2003
14	December 2003
15	December 2003
16	December 2003
17	December 2003
18	December 2003
19	December 2003
20	December 2003
21	December 2003
22	December 2003
23	December 2003
24	December 2003
25	December 2003
26	December 2003
27	December 2003
28	December 2003
29	December 2003
30	December 2003
31	December 2003
32	December 2003
33	December 2003
34	December 2003
35	December 2003
36	December 2003
37	December 2003
38	December 2003
39	December 2003
40	December 2003
41	December 2003
42	December 2003
43	December 2003
44	December 2003
45	December 2003
46	December 2003
47	December 2003
48	December 2003
49	December 2003
Appendix A 1	December 2003
Appendix A 2	December 2003
Appendix A 3	December 2003
Appendix A 4	December 2003
Appendix A 5	December 2003
Appendix A 6	December 2003
Appendix A 7	December 2003
Appendix A 8	December 2003
Appendix A 9	December 2003
Appendix A 10	December 2003

Contents

Foreword

The research reported in this Paper was funded by the Safety Regulation Group of the UK Civil Aviation Authority, and was performed by Cranfield Aerospace Ltd and the CAA Institute of Satellite Navigation at the University of Leeds. The work comprises a study of the effect of helicopter rotors on GPS reception which was highlighted as an issue for investigation during the flight trials of DGPS guidance for helicopter approaches to offshore platforms reported in CAA Paper 2000/5. Further impetus was added by the results of the third of the three follow-on trial studies reported in CAA Paper 2003/2 which identified a significant difference between the number of satellites tracked and those which were expected to have been tracked; the evidence available indicated the most likely cause to be the tail rotor (the GPS antenna had been mounted on the tail fin on the trials aircraft).

The CAA accepts the results of the study which will be taken into account in overseeing the use of GPS in helicopter operations, for which the most significant use is currently offshore en-route navigation. The GPS antennas on all helicopters currently operating in the North Sea region are understood to be located on the tail boom under the main rotor. The results of this study suggest that such installations may be expected to be less susceptible to the rotor effects identified and, based on the favourable in-service experience to date, this appears to be the case. However, little or no objective data for in-service operations exists, and it is noted that most of this experience is based on a GPS space segment with more satellites and a higher signal strength than that guaranteed by the system provider (US DoD).

In view of the foregoing, and in line with the recommendations contained within this Paper, CAA proposes to pursue two courses of action:

i) Establish a requirement and a means of compliance for confirming the acceptability of GPS antenna installations on helicopters. It is anticipated that this will take the form of a ground test procedure for use by helicopter operators and/or helicopter manufacturers in validating both existing and new antenna installations.

ii) Establish a practical means of monitoring GPS performance in order to detect any significant degradation. This may involve monitoring of the GPS space segment at a fixed location and/or monitoring of overall performance on board helicopters during routine operations.

Safety Regulation Group

December 2003

Effect of Helicopter Rotors on GPS Reception

1 Introduction

This report describes the results of a series of experiments undertaken in October 2002 on behalf of the UK Civil Aviation Authority (CAA) to investigate the effect of helicopter rotor blades upon the reception of GPS signals.

The experiments involved the installation of two GPS antennas and three dissimilar GPS receivers on a Sikorsky S76C helicopter operated by CHC Scotia Helicopters Ltd. A series of ground runs was undertaken during which the rotational speed of the helicopter rotors was varied in a controlled manner whilst monitoring the operation and performance of the GPS receivers.

The S76C airframe in question had previously been employed for a series of Differential GPS test flights sponsored by the CAA, the results from which (references [1], [2]) had revealed various interference issues which were suspected to be related to the presence of the helicopter rotors. The effects attributed to the rotors had included discrepancies between the number of available GPS measurements and those determined to be available from the satellite predictions, and significant reductions in the carrier-to-noise figure reported by a particular GPS receiver. The carrier-to-noise loss had appeared to be up to 12dB for satellite signals passing through the tail rotor disc.

The dedicated rotor interference experiment was a joint undertaking by Cranfield Aerospace Ltd (Cranfield), who were the prime contractor on the previous DGPS flight trials, and the CAA Institute of Satellite Navigation (ISN) at the University of Leeds. An enhanced set of experimental equipment, comprising three different receiver types connected to a common antenna, was fitted to the original test aircraft in order to permit a more detailed investigation of the previously observed effects. Data was collected using antenna locations adjacent to both the main and tail rotors, and incorporating variations both in rotor speed and in satellite positions relative to the aircraft.

This report, which has been prepared jointly by Cranfield and the ISN with additional input from the CAA and from Lambourne Navigation Ltd, begins (Section 4) with a description of the trials airframe, the experimental equipment and the test procedures employed.

The use of a proprietary GPS receiver designed by the ISN allowed the 'interference' effect to be sampled at a much higher rate than is possible with standard commercial receivers. This provided an important insight into the nature of the effect at a very low level within the receiver to characterise the interference phenomenon. The results from an analysis of this data are presented in Section 5.

Sections 6 and 7 present a summary of the effect of the rotors upon the accuracy and availability, respectively, of the satellite pseudorange measurements employed by the commercial GPS receivers. This is followed in Sections 8 and 9 by a discussion of the significance of the trial results and their impact upon the airworthiness of GPS installations on rotary wing aircraft.

Appendix A contains material relating to an analysis of the signal level (carrier-to-noise) estimates output by the GPS receivers when operating in the rotor 'interference' environment.

2 References

1 CAA Paper 2000/5, "DGPS Guidance for Helicopter Approaches to Offshore Platforms", CAA, 2000.

2) LNL/C06/058/R, "Further Analysis of the Flight Trials Data - Effects of Satellite Unavailability and Analysis of Receiver Tracking Performance", Lambourne Navigation Ltd, 2001.

3) SA 4047-76-5, "S76 Composite Materials Manual", Sikorsky, 1992.

4) S. Riley, "An Integrated Multichannel GPS/GLONASS Receiver", Proceedings of ION GPS-92, The Institute of Navigation, September 1992.

5) Advisory Circular 20-138, "Airworthiness Approval of GPS Navigation Equipment for use as a VFR and IFR Supplemental Navigation System", FAA, 1994.

6) A. J. Van Dierendonck, "GPS Receivers" in Parkinson, B. W. and Spilker, J. J. (Eds.) / Axelrad, P. and Enge, P. (Assoc. Eds.), Global Positioning System: Theory and Applications Volume I, Progress in Astronautics and Aeronautics Volume 163, pp329-407, 1996.

7) J. J. Spilker, "Digital Communications by Satellite", Prentice-Hall, 1977.

8) J. J. Spilker Jr, "Signal Structure and Theoretical Performance" in Parkinson, B. W. and Spilker, J. J. (Eds.) / Axelrad, P. and Enge, P. (Assoc. Eds.), Global Positioning System: Theory and Applications Volume I, Progress in Astronautics and Aeronautics Volume 163, pp57-120, 1996.

9) United States' Department of Defense, "Global Positioning System Standard Positioning Service Performance Standard", October 2001.

3 Abbreviations

ADR	Accumulated Delta Range
C/A	Coarse/Acquisition
CAA	UK Civil Aviation Authority
CNR	Carrier-to-Noise Ratio
Cranfield	Cranfield Aerospace Ltd
dB	Decibel
DC	Direct Current
DGPS	Differential Global Positioning System
DoD	Department of Defense
DSP	Digital Signal Processor
FAA	Federal Aviation Administration
FDR	Flight Data Recorder
FD RAIM	Fault Detection RAIM
GLONASS	Russian GNSS system
GNSS	Global Navigation Satellite System
GPS	Global Positioning System
HOMP	Helicopter Operational Monitoring Project
Hz	Hertz
IFR	Instrument Flight Rules
I_P	In-phase punctual correlation measurement
ISN	CAA Institute of Satellite Navigation, University of Leeds
m	Metre
Navstar	Navstar Systems Ltd
Nr	Rotor speed
PC	Personal Computer
PRN	Pseudo-Random Noise (GPS satellite identifier)
Q_P	Quadrature-phase punctual correlation measurement
RAIM	Receiver Autonomous Integrity Monitoring
RAM	Random Access Memory
RF	Radio Frequency
rpm	Revolutions per Minute
Rx	Receiver
s	Second
SBAS	Satellite Based Augmentation System
SIS	Signal-in-Space
Trimble	Trimble Navigation Ltd
TSO	Technical Standard Order
UK	United Kingdom
UTC	Universal Time Co-ordinated
VFR	Visual Flight Rules
o	Degree
Ω	Ohm

4 Experimental Procedure

4.1 Trials airframe

The rotor 'interference' experiment was performed using the Sikorsky S76C helicopter registration G-SSSC operated by CHC Scotia Ltd (formerly Bond Helicopters). This same aircraft had been employed for the earlier series of CAA-sponsored DGPS test flights and was considered to be representative of the small to medium-size helicopters currently in use for North Sea offshore support operations.

Suitable installation locations for GPS antennas on helicopters are, necessarily, relatively limited owing to the shape of the airframe. In the majority of cases it is not possible to ensure that the line-of-sight signal path to the GPS satellites will always be kept clear of the regions swept by the rotor blades, particularly since the direction of signal reception varies with the orbital motion of the satellites and with airframe attitude and heading changes in flight.

On G-SSSC, an existing antenna is presently located close to the midpoint of the tailboom which is used by the aircraft's 'normal' GPS receiver. As may be observed from Figure 1, in this position the antenna is below the main rotor disc and is also close to the tail rotor. Installation of GPS antennas in similar locations appears to be common on several other UK offshore aircraft: for example, Figure 2 shows the antenna position on a Super Puma aircraft operated by Bristow Helicopters Ltd.

Figure 1 GPS antenna locations on Sikorsky S76C G-SSSC

Figure 2 GPS antenna location on Super Puma G-TIGE

Rather than disturbing the existing flight-cleared GPS equipment on G-SSSC, two additional antennas were temporarily installed in positions (Figure 1) which had been employed for the earlier trials [1]. Both antennas were Aeroantenna Technology model AT575-12, incorporating an integral 26.5dB preamplifier.

One of these GPS antennas was installed at the top of the vertical tail, in a position immediately adjacent to the tail rotor (which is positioned on the port side of the aircraft). Ignoring any coning effects, this antenna was above the plane of the main rotors. The second GPS antenna was installed on the fuselage nose immediately forward of the cockpit windows, below the main rotor disc.

The re-use of these two antenna positions was partly dictated by the desire to replicate the 'interference' effects which had been observed on the previous trials, but it also provided good geometry for investigating the effect on GPS satellite signals when passing through either the main rotor (nose antenna) or tail rotor (tail antenna).

4.2 Rotor blade construction

Both the main rotor and tail rotor on the S76C comprise four blades and rotate at a nominally constant speed in flight. However, the rotation rates are different:

Main rotor: 313 rpm

Tail rotor: 1723 rpm

The rotor speed (Nr) is displayed to the pilots in the form of a percentage value, with the above rates represented as 107% Nr (the rotor speeds on the S76C are 7% greater than those employed on Sikorsky's earlier S76A model). When running at 107% Nr, the interval between the passage of successive blades is shown to be 48ms for the main rotor and 9ms for the tail rotor.

Both the main and tail rotor blades are of composite construction, as shown in Figure 3 and Figure 4 overleaf which are reproduced from [3]. Being constructed from a combination of materials whose electromagnetic properties such as dielectric constant and conductivity are different from those of the surrounding air as well as from each other, the propagation of an RF signal in the vicinity of a blade will be affected via a series of processes (including reflection, refraction and attenuation) which are normally impracticable to analyse through theoretical means alone.

The philosophy behind the rotor 'interference' experiment was therefore to undertake an empirical assessment of the effect of some typical helicopter rotor blades upon the operation of several different GPS receivers, as a function of various parameters (such as relative geometry and rotor speed) which could be readily controlled. It was anticipated that the results from this process would provide additional insight into some of the anomalous effects previously observed, and might also form the basis for recommendations or guidance relating to the certification of GPS equipment on rotary wing aircraft.

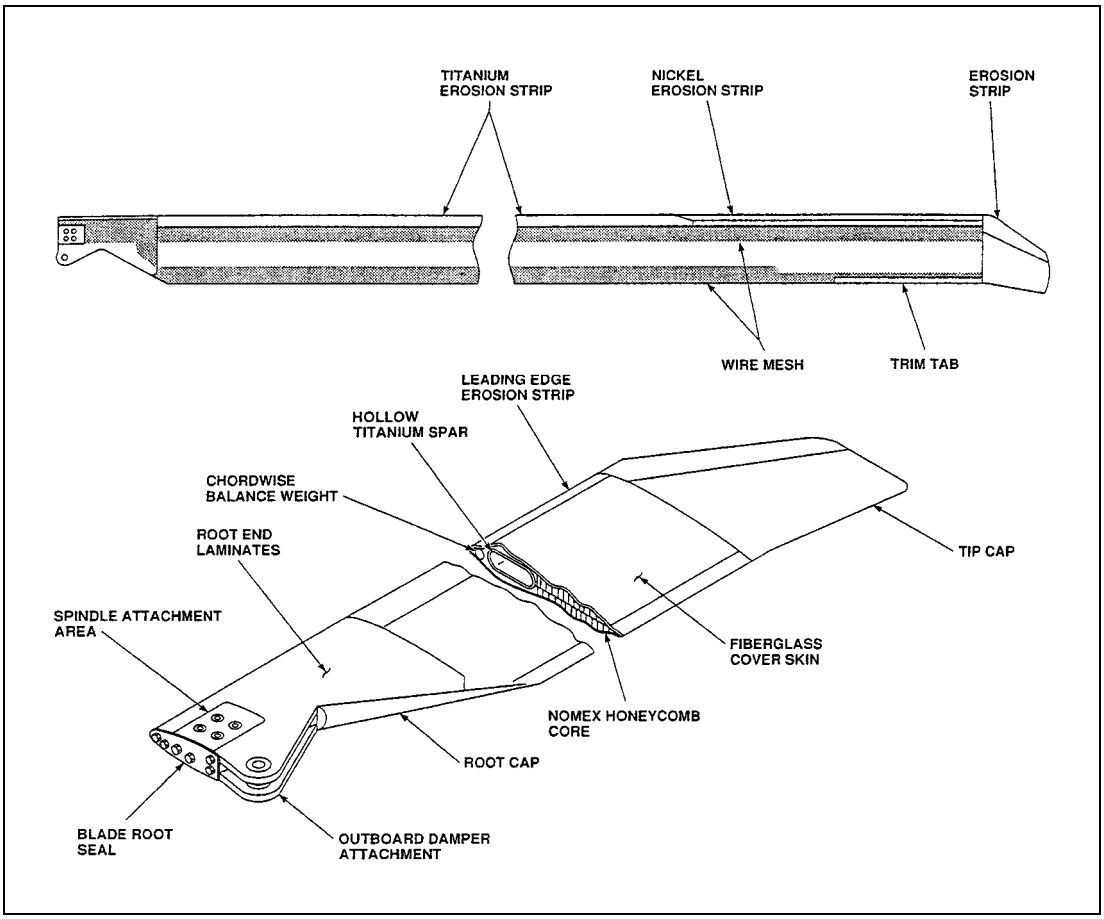

Figure 3 Main rotor blade construction (from [3])

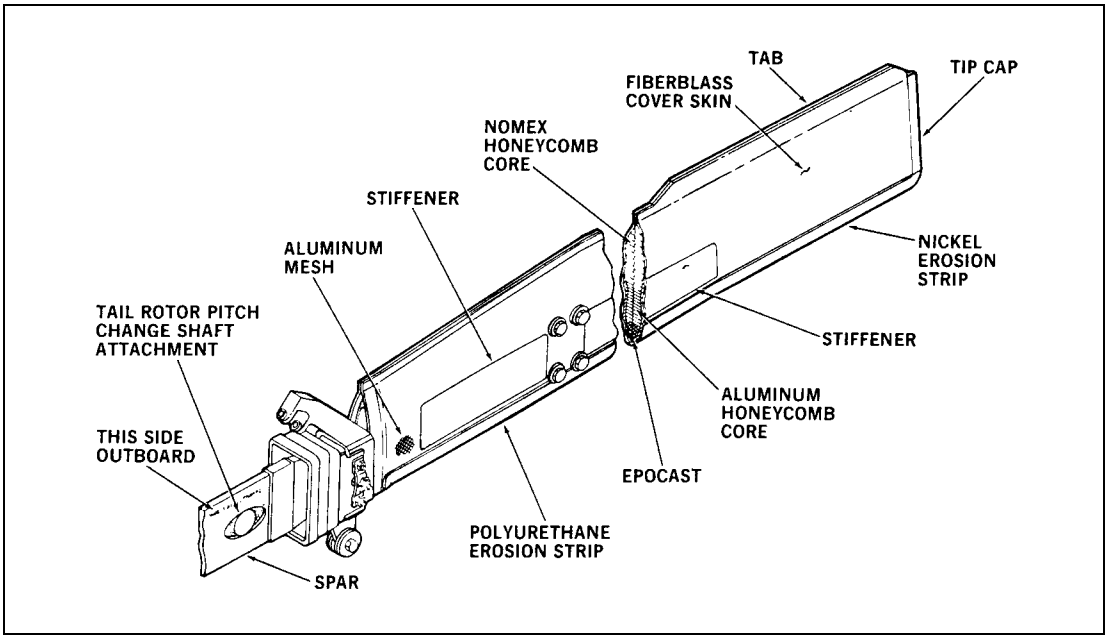

Figure 4 Tail rotor blade construction (from [3])

4.3 Test equipment

A block diagram of the experimental equipment installation is shown in Figure 5. Although two different GPS antenna positions (nose and tail) were available, only one was used at any one time with the selection between the two being undertaken manually. The output from the selected GPS antenna was fed to a preamplifier/splitter arrangement which was identical to that employed for the earlier DGPS test flights [1].

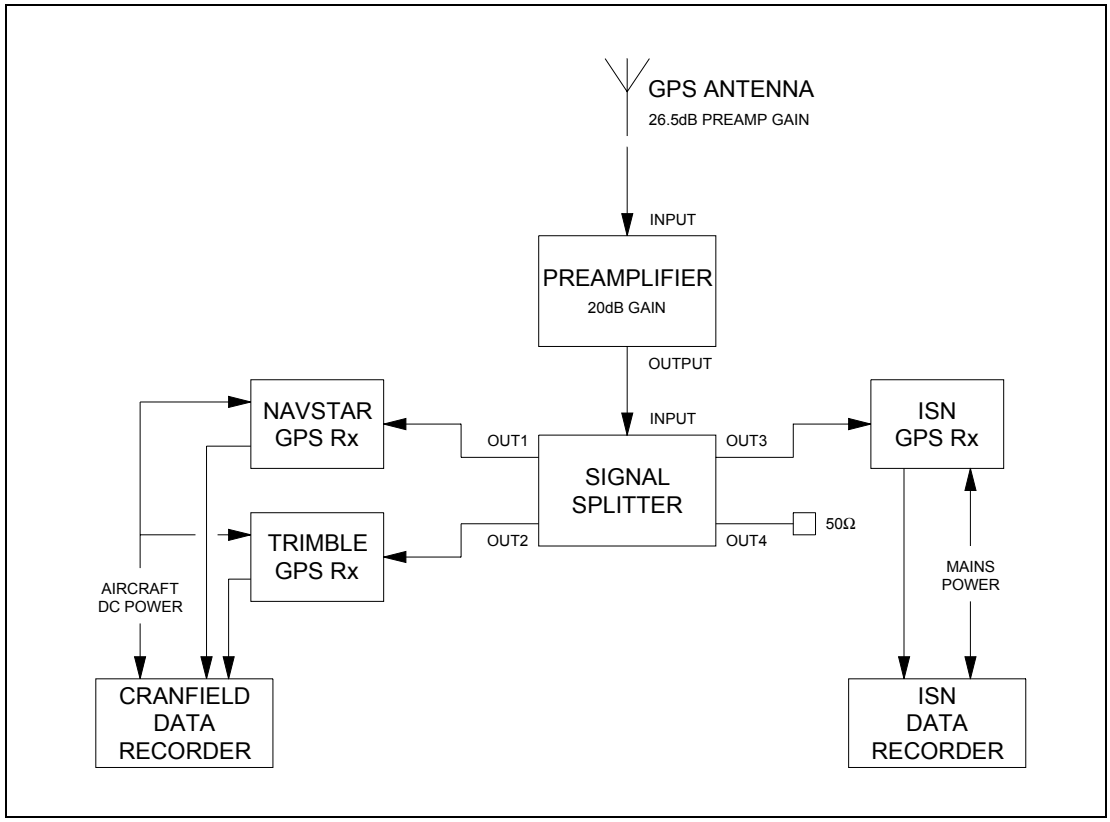

Figure 5 Experimental equipment configuration

This arrangement provided separate RF feeds for three independent and dissimilar GPS receivers, two of which had previously been employed on this aircraft:

a) Navstar Systems Ltd XR5-M12

This receiver is a ruggedised C/A code GPS 'engine' capable of tracking up to twelve satellites. The unit was identical to that employed on the earlier trials, with the exception that the internal firmware had been updated in the interim to provide Year 2000 compatibility. The XR5-M12 is not certified to any recognised civil airborne standard (such as TSO-C129).

b) Trimble Navigation Ltd TNL-2100

This system was identical to that used for the earlier trials and is a modified version of the TSO-C129 compliant Trimble TNL-2100T C/A code receiver, capable of tracking up to eight satellites. The software modification provides the receiver with the ability to accept differential corrections and is not believed to affect its signal tracking performance. The Trimble installation incorporated an RF circulator, as described in [1], which had been shown to be necessary to avoid interference to the other receivers when operating from a common antenna.

c) ISN 20 channel GPS/GLONASS receiver

This receiver is one of a number of high performance survey quality systems developed in their entirety at the ISN. The receiver is capable of tracking any combination of GPS and GLONASS C/A code signals and it outputs high precision code and carrier phase measurements. In addition, as the receiver was developed at the ISN as a high performance instrument for GNSS research purposes, it is also able to output very low level information, such as correlator totals, which is rarely available from commercial receivers. The ISN receiver has not been certified to TSO-C129. Further details regarding its architecture and performance can be found in [4].

The power source for the GPS receivers and the associated recording equipment was derived from the onboard aircraft DC supplies in the case of the Cranfield equipment, and from an external mains supply in the case of the ISN equipment.

Real-time data from each GPS receiver was recorded at a 1Hz rate synchronised to GPS time. In addition the ISN receiver included a facility which allowed fast sampling to be performed on demand from the tracking correlators associated with particular satellite channels, at rates of up to 1kHz. This feature is described in more detail in Section 5.

One of the primary requirements for the trial was to be able to monitor the GPS receivers' ability to perform a range measurement on each satellite in view in the presence of 'interference' from the rotor blades. Accordingly, the recorded data from each receiver included, as a minimum, a tracking status flag and a measure of the received signal level for each channel. The Navstar and ISN receivers also provided code and carrier measurement observables together with azimuth and elevation data for the satellites.

Other data from the GPS receivers (such as the position and velocity estimates from the navigation solution filters) was also recorded but was not employed in the subsequent analysis.

Following completion of the trial, the contents of the aircraft Flight Data Recorder memory was downloaded to provide a recording of the rotor speed (Nr) and magnetic heading as a function of time. Owing to the lack of direct synchronisation between the FDR timebase and UTC time, a post-flight correction based on manual observations was applied to align the FDR and GPS recordings to an accuracy of better than ±2s.

The accuracy of the Nr measurements was stated by CHC Scotia to be better than ±1%. Knowledge of the aircraft true heading based upon corrected FDR data is believed to be better than $\pm 5^{o}$, the dominating uncertainty being the local magnetic variation.

4.4 Test procedure

The experiment was undertaken at Aberdeen (Dyce) airport on the 12th October 2002. The aircraft was parked in an area on the CHC Scotia apron on the northwestern side of the airport, at least 60m from the nearest building and from other potential sources of interference. The weather conditions during the trial were wet, with heavy rain at times.

The aircraft heading was varied over the course of the trial (either by ground taxying whilst the rotors were running, or through ground handling with a tug vehicle) in order to ensure that the relative position of the GPS satellites was appropriate to the test being undertaken. This was achieved by referring to a printout of satellite predictions based upon almanac data, which showed azimuth and elevation for each PRN as a

function of time. The actual satellite positions were also confirmed in real time during the trial.

The tests comprised the activities described below which were undertaken with the experimental equipment connected to both the tail and nose antenna installations. Correct positioning of the aircraft was particularly important in the case of the tail antenna tests where it was a requirement to ensure that the signal path from at least one satellite to the antenna always intersected the tail rotor disc.

a) Manual rotations of the rotor blades

   With the aircraft engines stopped and the rotor brake disengaged, the rotors were turned slowly by hand so that successive blades would intersect the signal path from appropriate satellites to the antenna. Care was taken to ensure that the engineer turning the blades was positioned well away from the antenna.

b) Rotor start/stop sequences

   The aircraft engines were used to spin the rotors up to the normal operating speed of 107% Nr. Following a period of constant speed running at 107% (generally for 1-2 minutes, although two test periods in excess of 20 minutes were also undertaken with the tail antenna), the rotor speed was reduced back to zero.

   A normal rotor start sequence with the S76C is performed by starting one of the two engines and allowing the rotor speed to increase to the ground idle setting of approximately 60-70% Nr. The second engine is then started and coupled to the drivetrain before the speed is increased to 107%. When stopping the rotors a similar procedure is performed in reverse, with the speed being reduced initially to ground idle and subsequently to zero. The time to perform a complete start sequence is typically of the order of 60-70s, and that for a stop sequence slightly less.

By following similar procedures on each of the test runs, it was intended that the resulting GPS data would allow the variation of any 'interference' effect with Nr to be investigated, whilst reducing the impact of any external factors such as satellite azimuth/elevation changes due to orbital motion.

5 Effect of Rotors on Signals-in-Space

5.1 ISN receiver 'snapshot' facility

The ISN receiver is a highly flexible instrument that can be modified to provide different signal processing strategies, and also to provide access to low-level information such as correlator totals. This allows a thorough examination of received GPS signals to be carried out using known receiver processing. For the experiments performed in this trial it was desirable to be able to examine the effect (if any) of the rotors on the received signal, at a rate considerably higher than that provided by standard commercial receivers. The ISN receiver was therefore to be used as an instrument to determine the effect of the rotors on the signal-in-space (SIS). The ISN receiver was modified to output correlation data at a variety of sample rates, as will be detailed. Prior to this a brief overview of the configuration of the ISN receiver and the correlation measurements it produces is given.

The ISN receiver comprises the following key subsystems:

- Analogue processing chain to amplify, filter and frequency translate the received signal prior to digital sampling.

- Analogue to digital converter, which converts the analogue signal to a 1-bit digital representation at a frequency of 20MHz; both in-phase (I) and quadrature-phase (Q) samples are produced.
- Digital hardware which performs a digital frequency mix to baseband, followed by de-spreading of the signal through correlation with locally generated versions of the spreading pseudo-random noise (PRN) code.
- A digital signal processor (DSP) that controls the receiver hardware. The DSP processes the correlation totals produced by the hardware and determines the feedback required by the hardware to track the signal.
- A PC is used to command the receiver to track the available satellites. The PC stores the data produced by the receiver, including all observables.

The ISN receiver uses a total of four correlation measurements to acquire and track the incoming signals. The integration period used is 1ms. Each correlation measurement indicates the degree of alignment of the locally generated version of the PRN code used for de-spreading, together with the alignment of the carrier frequency and phase used to frequency translate the incoming signal to baseband. Correlation involves comparing the incoming and local PRN codes on a sample by sample basis. The net number of agreements minus disagreements is produced as the correlation count. These counts are the correlation totals that will be referred to in the remainder of this document.

In order to align the incoming and local PRN codes three time delayed versions of the local code are generated; these are known as early(E), punctual(P) and late(L), with the early-punctual delay being the same as the punctual-late delay. The receiver tracking acts to align the punctual correlator with the incoming signal. In order to track the incoming signal in frequency and phase, both the in-phase and quadrature-phase versions of the incoming signal are processed; hence both I and Q correlation measurements are produced. In order to track the incoming signal phase all energy is tracked into the I channel. Therefore the correlation measurements used in the ISN receiver are I_E, I_P, I_L and Q_P; i.e. in-phase early, punctual and late measurements for code tracking, and quadrature-phase punctual measurements that are used for carrier tracking along with I_P. When in steady state the I_P correlation measurement should have maximum signal energy, whilst the Q_P correlator should contain zero mean Gaussian noise only.

The DSP used in the ISN receiver has unused on-board RAM that can be used to store approximately 10,300 32-bit data words. It was decided that the snapshot facility should use this RAM space to store the 1ms correlation totals in real-time. These correlation totals are from a single satellite at a time, in order to capture a significant number for analysis. Once the RAM space is full the data should then be sent to the PC for storage. The 1ms ISN correlator totals are truncated to 10 bits within the receiver without adversely affecting the tracking accuracy. When storing 1ms I_P and Q_P correlation totals only 20 bits of data need be stored for each measurement, which will clearly fit into a single 32-bit word. The spare 12 bits can be used to store correlation totals that are produced over longer integration periods. Hence the receiver was configured to store 1, 2, 4, 8, 16, 32 and 64ms correlation totals. The 10,300 storage spaces in the RAM are therefore filled after 10.3 seconds when logging 1ms correlation totals, 20.6 seconds when logging 2ms totals etc.

Once a signal has been acquired by the receiver a snapshot can be taken; the correlation period to be used is selectable via the PC. Once the snapshot has been taken the data is automatically sent to the PC over approximately a 10s period. This period is used in order to prevent overloading the communications link between the

receiver and the PC, which must also continue to transport the standard observables for all other receiver channels that are tracking other satellites. Once this data transfer has completed the next snapshot can be taken. The PC stores the snapshot data with a time tag that relates to the time at which the first snapshot measurement was made. Hence the snapshot facility does not have an impact upon the standard receiver functionality. The receiver is still able to track satellites on 20 channels and produce observables at a 1Hz rate.

5.2 Snapshot data with rotors stationary

Before presenting the snapshot data obtained during the trials when the rotors were turning, it is important to first characterise the snapshot data when the rotor blades were stationary. Shown in Figure 6 are the punctual in-phase (I_p) and quadrature-phase (Q_p) correlation totals for PRN 28 during such a period. As stated in Section 5.1, the correlation totals used in the receiver are truncated counts of the net number of agreements over the number of disagreements, when comparing the incoming and local PRN codes. The correlation totals can therefore be considered to be scaled amplitude measurements. For the purposes of this analysis the most important information to be gained from the correlation totals is their variation over time. Hence the correlation totals are presented solely in the form that they are output by the receiver.

To improve the clarity of the plot, the phase transitions caused by the GPS navigation data message that are produced in the I_p data have been removed by plotting the absolute value of the I_p correlation totals.

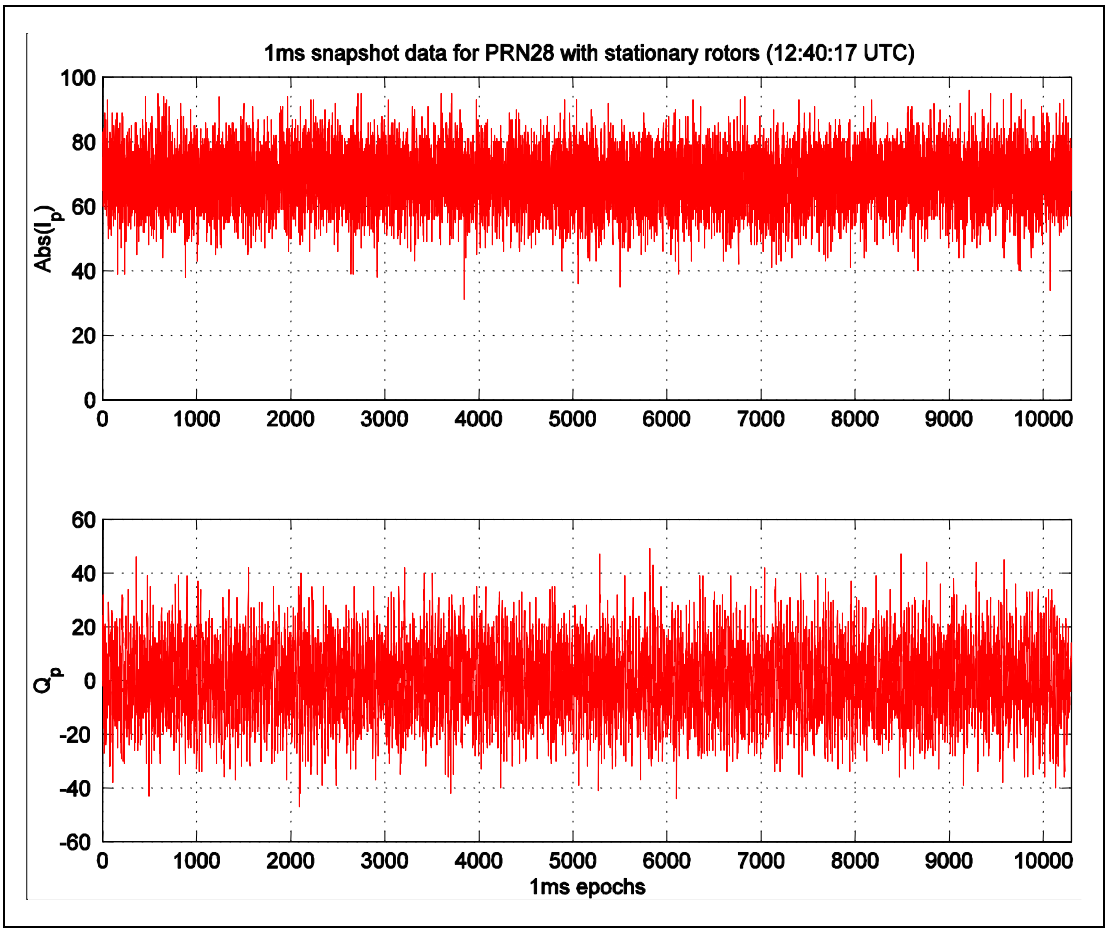

Figure 6 Snapshot data for PRN 28 with rotors stationary

As the receiver is carrier phase tracking all signal energy is in the in-phase channel, i.e. I_p, whilst the quadrature-phase channel contains zero mean Gaussian noise only. This snapshot data profile is typical of those captured during periods when the rotors were stationary, as will be shown in this section. They are also typical of the profiles obtained at a stationary antenna location at the University of Leeds. The absolute level of the I_p correlation totals is dependent on the received signal power, which is most commonly represented in terms of the carrier to noise ratio (CNR). The variance of both the I_p and Q_p correlation totals are also dependent on the CNR. The CNR is a function of satellite transmit power, the satellite antenna gain pattern, atmospheric path losses, the receive antenna gain pattern and also the implementation losses imposed by the receiver architecture and implementation used. Hence, unless the different implementation losses are accounted for, the CNR as measured by two different receivers will be different. The CNR calculated by the ISN receiver does not account for implementation losses as these are difficult to estimate accurately, due to the time and temperature variation of components within the receiver. The CNR calculated is that within the tracking loops only. The technique used in the ISN receiver to produce CNR estimates at a 1Hz rate is that detailed in [7].

The captured high rate I_p and Q_p snapshot data can also be used to estimate the CNR, as measured within the tracking loops. There are a number of techniques that can be used to form the CNR; some require knowledge of the background noise power whilst others work only for single bit sampling receivers. The technique that has been used in this work to estimate CNR from the snapshot data is that detailed in [6], which does not require a background noise power measurement and can be used with different input sample resolutions. Also it requires simply I_p and Q_p measurements which are the core snapshot data that was captured. The technique involves the calculation of signal-plus-noise power in two different noise bandwidths; a wide band and a narrow band. A detailed description of the technique is outside the scope of this report and so shall not be given here. Using this CNR estimator (configured with M=20 and K=50) ten 1s CNRs were formed for the 10s worth of snapshot data. The mean CNR was 42.7dBHz, the variance of the ten CNRs was very small. The approximate elevation angle of the satellite at this time was 45^o.

The frequency response of the snapshot data can also be analysed in order to investigate if there are any deterministic structures within the correlation total data. The technique that has been used has been to determine the spectrum of the envelope of the received signal. That is, in the time domain the quantity $P(t)=I_p^2+Q_p^2$ has been formed. The spectrum of P(t), denoted P(f), has then been formed using a discrete Fourier transform. As the correlation totals were produced at a rate of 1kHz in this case, the spectrum produced will allow signal components at frequencies up to 500Hz to be identified. The resolution of the spectral data is 0.1Hz, as 10s of data was used. The spectrum for the PRN 28 data set shown previously in Figure 6 is given in Figure 7. To aid presentation the y-axis of the plot has been limited to the value shown (the signal component at DC extends to a value of 5×10^7).

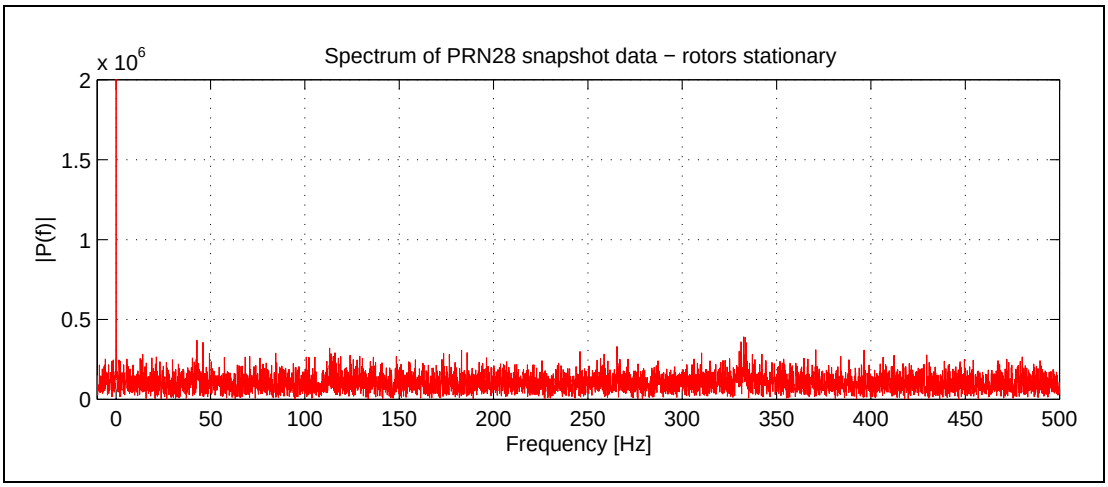

Figure 7 Spectrum of PRN 28 snapshot data with rotors stationary

Other than the signal component at DC, there are no significant frequency components present in the data. The signal component at DC is due to the fact that the envelope of the received signal has a non-zero mean. The essentially flat spectrum shown is indicative of the fact that the incoming signal dynamics are being successfully tracked by the receiver. The only envelope perturbations remaining are due solely to noise.

In order to further characterise the snapshot data for periods when the rotors were stationary, data from three other satellites are presented. In Figure 8 are the I_p and Q_p data for PRN 8. All signal energy is being tracked in the in-phase channel, with the quadrature-phase channel containing zero-mean Gaussian noise only. The spectrum of the PRN 8 envelope (P(f)), is shown in Figure 9. Again it is clear that there are no discernible deterministic signal components in the frequency range shown (other than DC). Use of the CNR estimator discussed previously results in an estimated CNR value of 41.4dBHz for PRN 8 during the time at which this snapshot was taken, when the satellite was at an elevation angle of approximately 27^{o}.

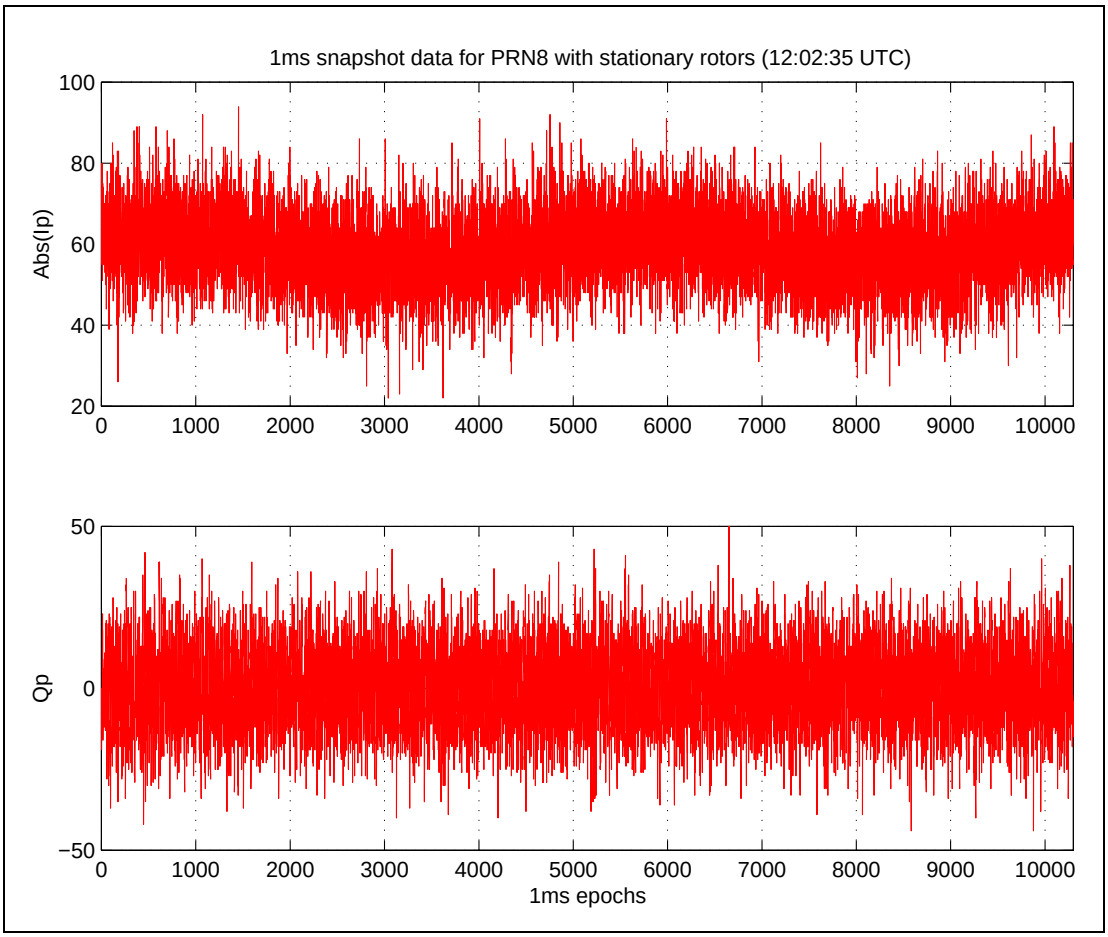

Figure 8 1ms snapshot data for PRN 8 with rotors stationary

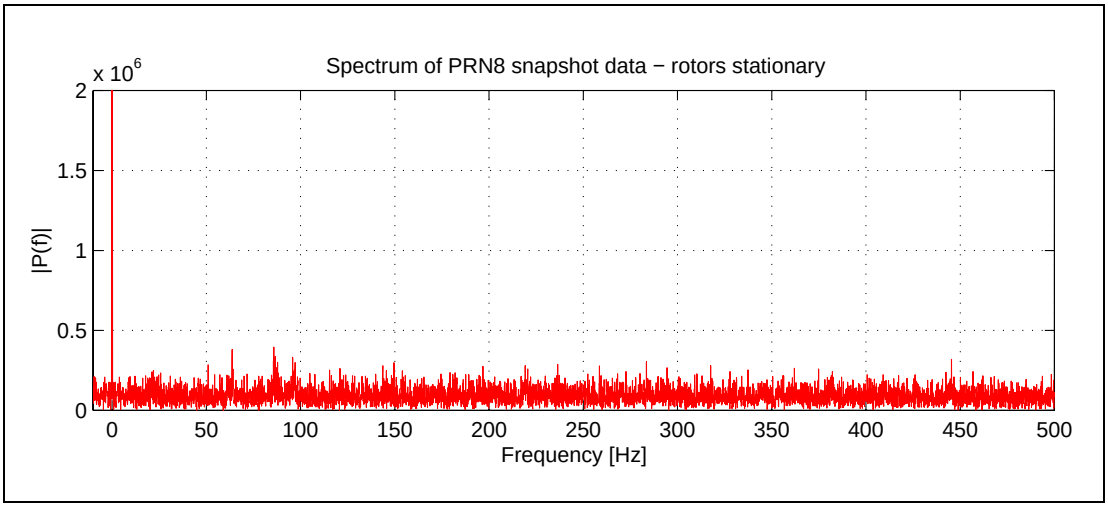

Figure 9 Spectrum of PRN 8 snapshot data with rotors stationary

The snapshot correlation data for PRN 9 is shown in Figure 10, and the corresponding frequency spectrum of that data is shown in Figure 11. Again it is clear that the signal is being accurately tracked into the in-phase channel. There are no detectable signal components at frequencies other than DC. For reference this satellite was at an approximate elevation angle of 42^{o}. The estimated CNR for this data set was 42.6dBHz.

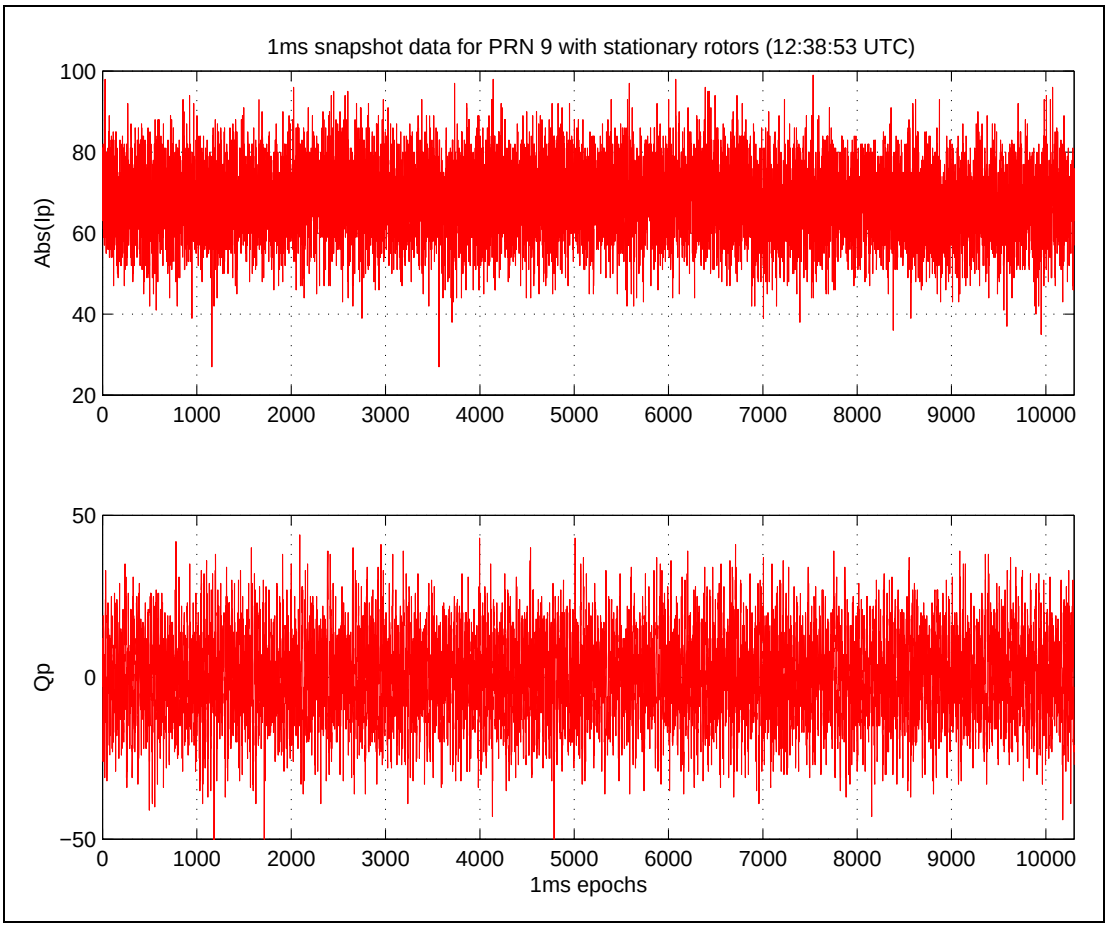

Figure 10 1ms snapshot data for PRN 9 with rotors stationary

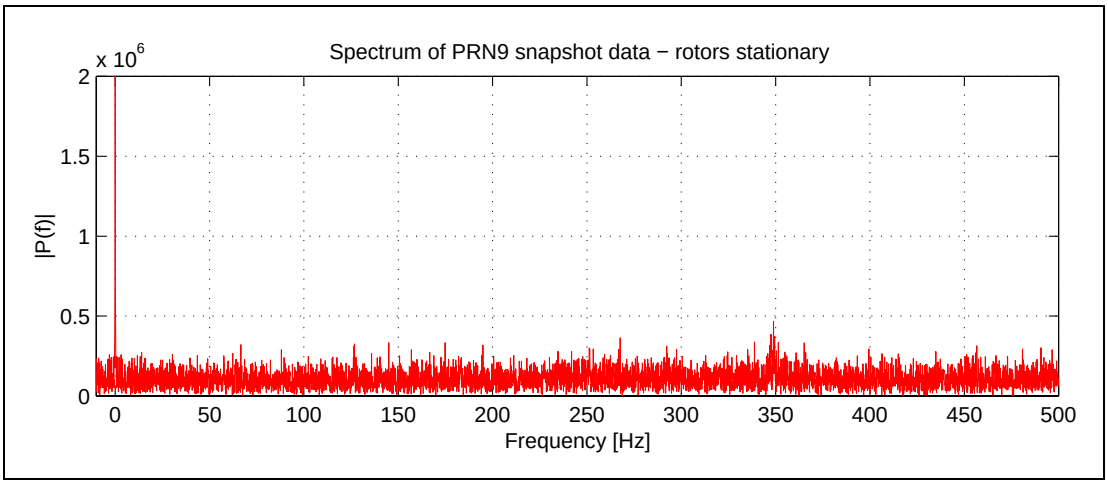

Figure 11 Spectrum of PRN 9 snapshot data with rotors stationary

The final snapshot data to be presented in this section is from PRN 30. The correlation totals are shown in Figure 12, whilst the spectral representation of that data is shown in Figure 13. The correlation data is very similar to that shown previously in this section for PRNs 28, 8 and 9. Again, there are no significant frequency components present in the envelope of the received signal other than at DC. The estimated CNR for this data set was 42.2dBHz. The satellite was at an elevation angle of approximately 26^{o}.

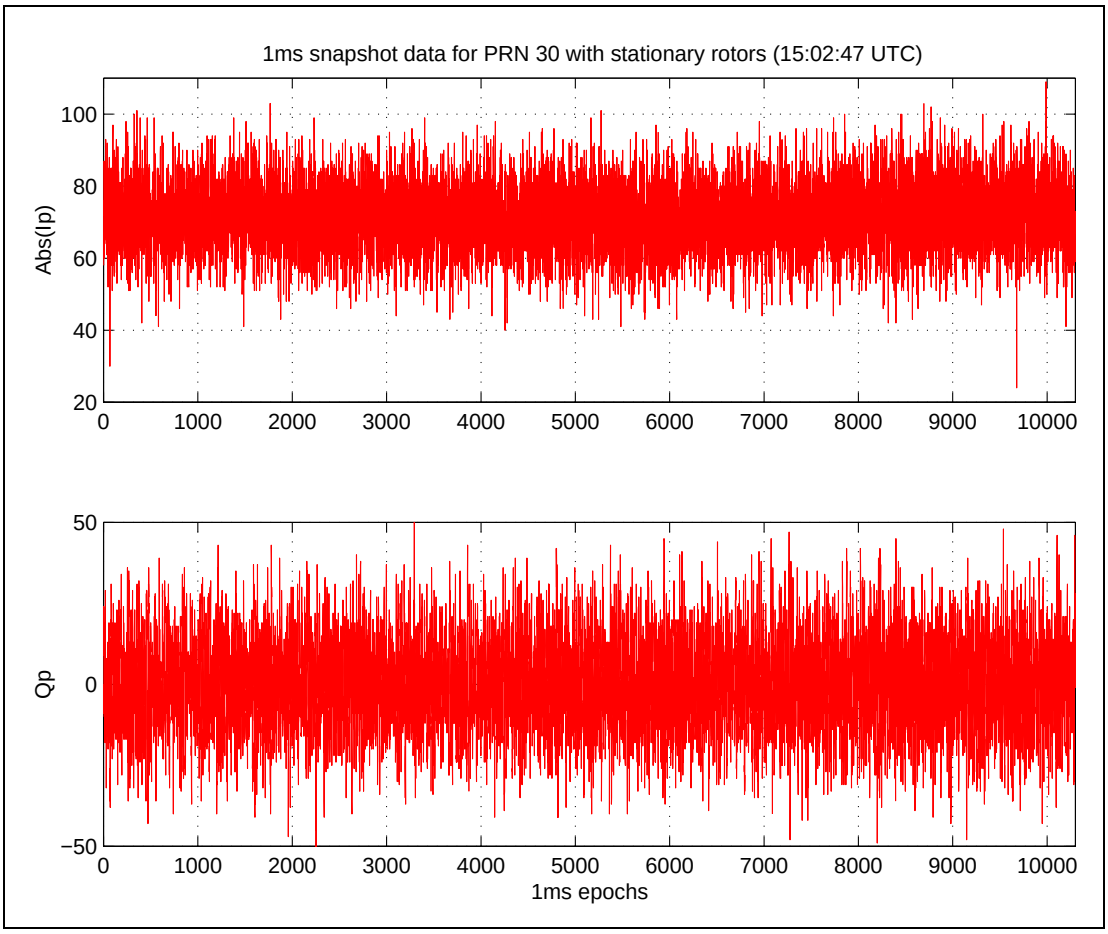

Figure 12 1ms snapshot data for PRN 30 with rotors stationary

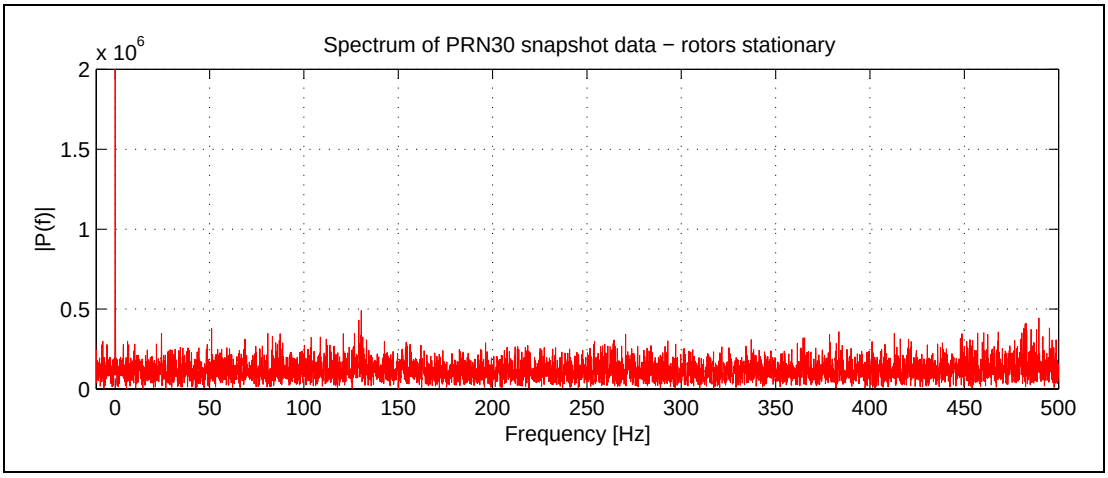

Figure 13 Spectrum of PRN 30 snapshot data with rotors stationary

Having characterised the snapshot data recorded by the ISN receiver aboard the aircraft during times when the rotors were stationary, the effects of non-stationary rotors on these correlation totals, for both the tail and main rotors, are now presented. The purpose of this is twofold. First it must be determined if the ISN receiver also suffers from the 'interference' effect observed during the previous trial. Second, if such 'interference' effects are produced the high sample rate data produced by the ISN receiver will allow a closer inspection of the phenomenon.

5.3 Snapshot data with rotors turning - tail rotor

The first snapshot data to be presented is from PRN 28 at a time when the rotors were turning at a speed of approximately 62.5% Nr. This speed is that recorded by the flight data recorder, which is reported to have an accuracy of ±1%. For the tail rotor 100% Nr corresponds to 1609rpm. The correlation data during this period of turning rotors is shown in Figure 14.

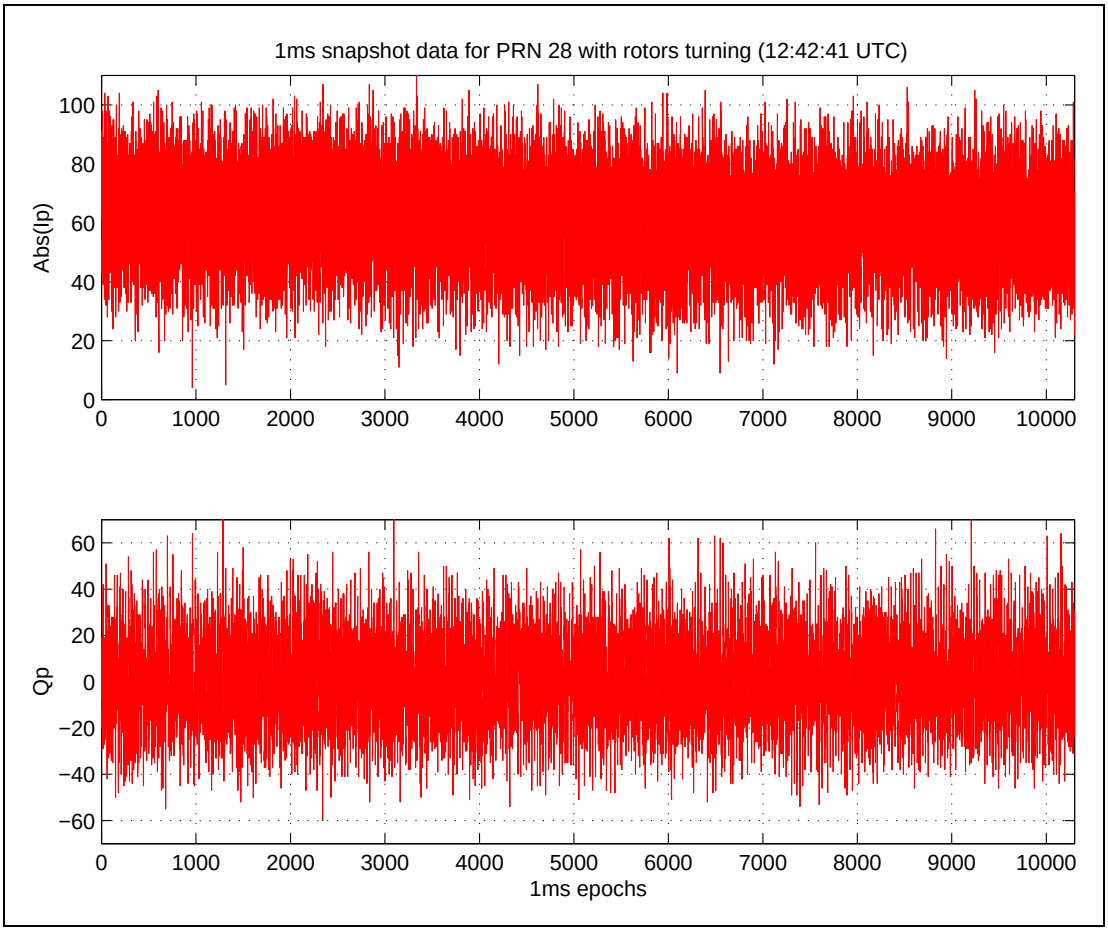

Figure 14 1ms snapshot data for PRN 28 with rotors turning at 62.5%Nr

This snapshot began only 2 minutes and 24 seconds after the start of the snapshot shown in Figure 6 when the rotors were stationary. The axes have been made as similar as possible to those used in Figure 6, in order to clearly demonstrate the effect the rotors have on the correlation data. The correlation data noticeably increases in variance when the rotors are turning. This is particularly the case for the I_p data. Comparing the two data sets the standard deviation of the I_p data increases by almost a factor of two, whilst the standard deviation of the Q_p data increases by 43%. The most obvious reason for an increase in variance would be that the received signal power had reduced. However, in that case it would be expected that the increase in the variance of the I_p and Q_p data would be more similar. Closer inspection of the correlation data is therefore required in order to determine the cause of the increased variance. The first 500ms of the I_p correlation data from Figure 14 when the rotors were turning at approximately 62.5% Nr, together with the first 500ms of data from Figure 6 when the rotors were stationary, are presented in Figure 15.

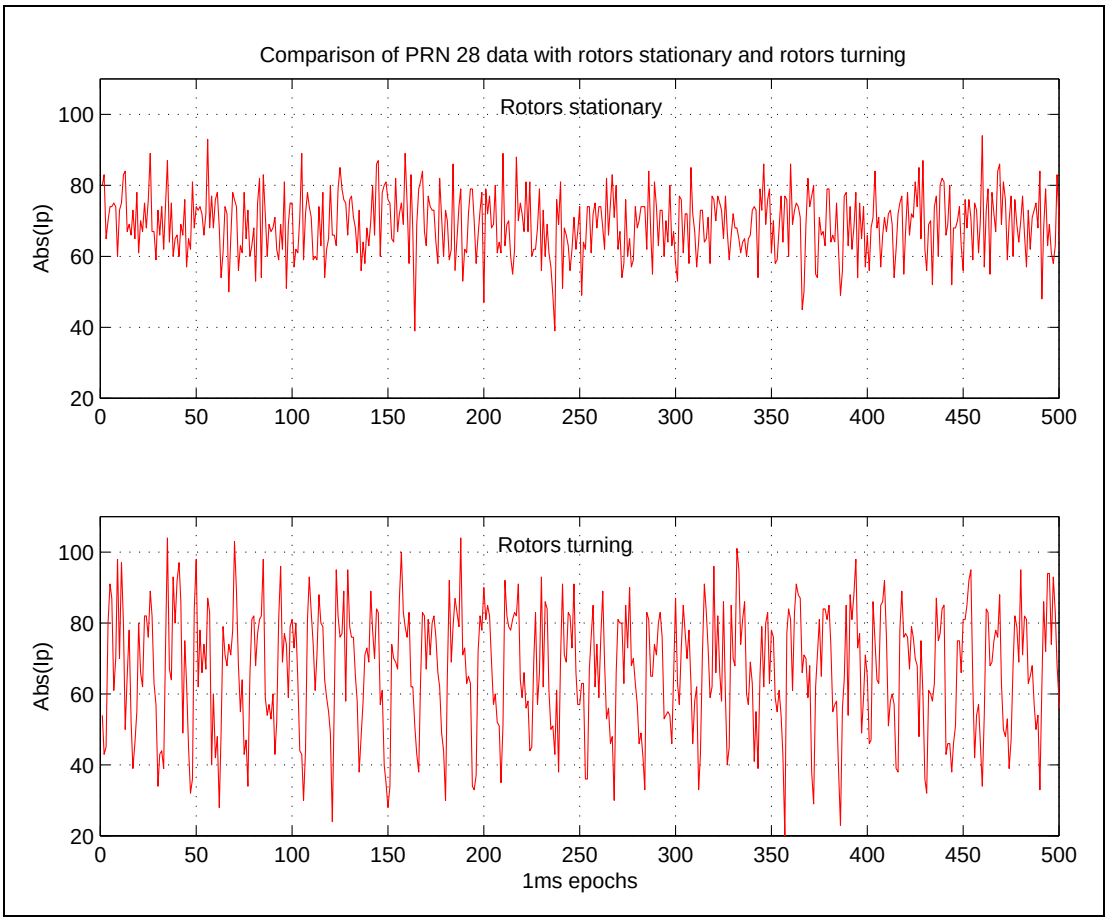

Figure 15 Comparison of PRN 28 snapshots with rotors turning and rotors stationary

The two data sets are clearly very different in nature. When the rotors are turning there are large oscillations produced in the in-phase data. Clearly these oscillations are exhibiting a deterministic nature, which is not evident in the data when the rotors are stationary. The spectra of the correlation data gathered when the rotors were stationary shown previously in Section 5.2 confirmed that no such deterministic structures were detectable in that data. The current data set shows that when the rotors are turning the signal is being tracked at approximately the expected level for the majority of the time, with the signal level then reducing rapidly for a shorter duration of time. The signal amplitude during these shorter periods would appear to be reduced by a factor of approximately 50%. Overall the estimated CNR for this data set is 37.5dBHz, some 5.2dB below that for the data set shown previously in Figure 6. As already stated, that data set was taken only 2 minutes and 24 seconds prior to the current data set, hence 5.2dB is a significant reduction in signal level over such a short period of time. Given that the signal is only being 'blocked' by the rotors for a small proportion of the time, as seen in Figure 15, the 5.2dB reduction is larger than expected. Further investigation of the performance of the CNR estimation technique is presented in Appendix A.

The observed oscillatory behaviour would suggest that the rotors are causing attenuation of the signal as they obscure the signal path. However, before investigating this theory further it is necessary to more fully characterise the observed oscillations. The spectrum of the received signal envelope for the data with the rotors turning is shown in Figure 16. It should be noted that, for clarity, the limits of the y-axis in the upper plot have been increased from those used in Section 5.2.

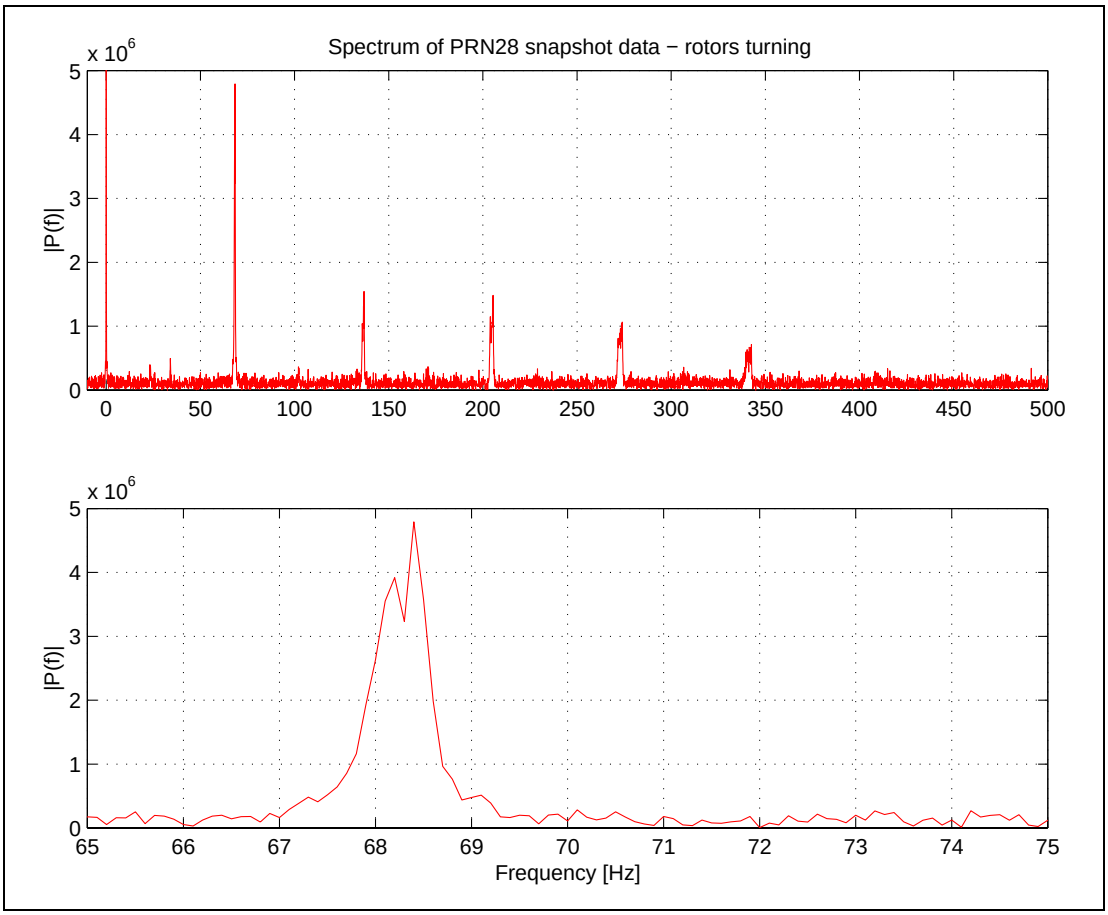

Figure 16 Spectrum of PRN28 data with rotors turning

In the upper plot there are clear frequency components in the spectrum of the snapshot data. It should be recalled that there were no such components in the data sets shown previously in Section 5.2 when the rotors were stationary. The largest frequency component (excluding that at DC) is shown in greater detail in the lower plot, where it can be seen to have a frequency of approximately 68.5Hz. In the upper plot it can be seen that the other large frequency components are harmonics of this 68.5Hz signal. For this data set the flight data recorder indicates that the rotor was turning at a speed in the range of 62.3% Nr to 63% Nr during the time of the data set. Therefore for the entire data set a mid point value to use would be 62.65% Nr. Given that 100% Nr equates to 1609rpm for the tail rotor, which has four blades, the blade passing frequency is given by:

$$\frac{0.6265*1609*4}{60} = 67.2\,\text{Hz}$$

Given the accuracy of the recorded rotor speed and the reference timebase, this value is clearly very close to the fundamental frequency of the oscillations observed in the correlation data. This result suggests that the oscillations observed in the correlation data are caused by the passage of the rotor blades between the antenna and the incoming signal wavefront.

Further evidence of the effect of the tail rotors on the correlation data is present in the correlation data for PRN 30. This data was recorded during a period when the rotor speed was held constant at a value of 74.5% Nr, and is presented in Figure 17. The frequency domain representation of the received signal envelope is also shown.

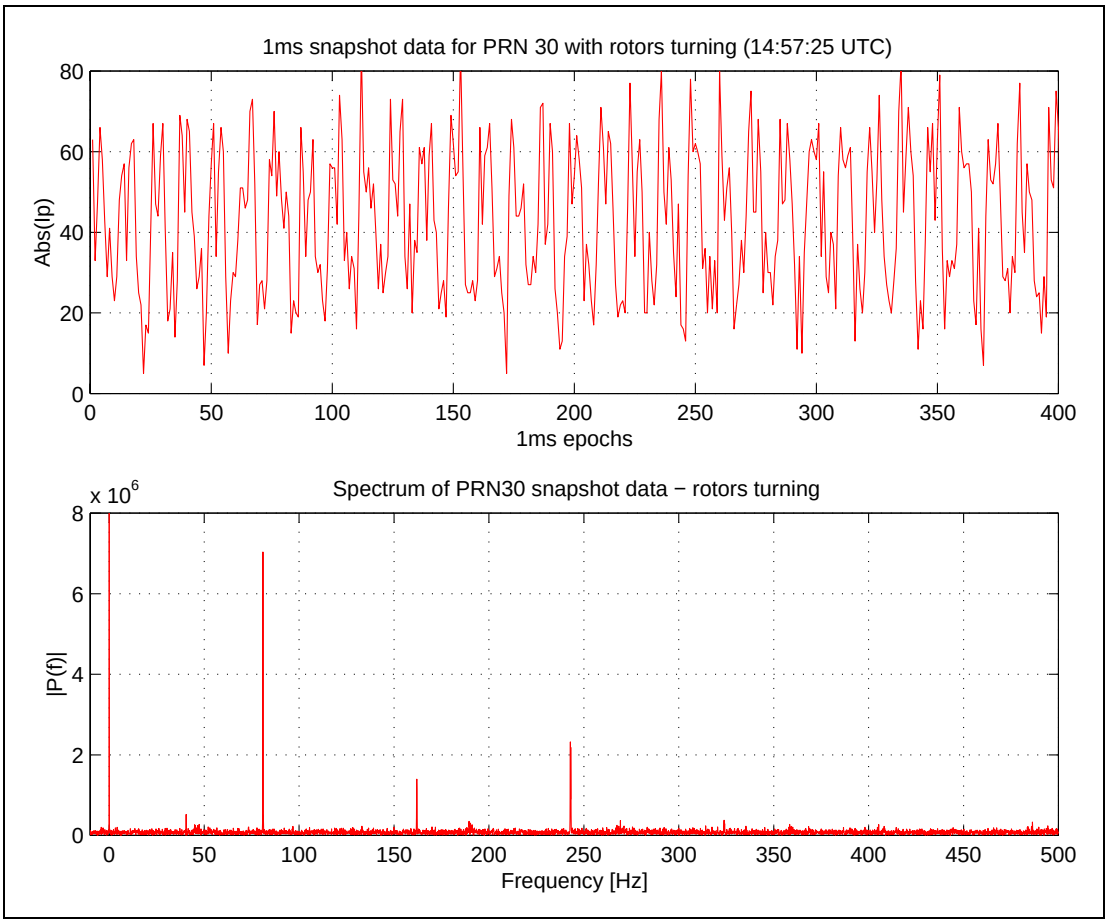

Figure 17 Snapshot data and frequency representation for PRN 30 with rotors turning

The correlation data again exhibits clear oscillations when the rotors are turning. The signal amplitude during the troughs in the waveform can be seen to be in the region of 50% relative to the average peak level. These oscillations were not evident in the correlation data for PRN 30 when the rotors were stationary, shown previously in Figure 12, which was recorded only 5 minutes later. The estimated CNR for this data set, which will be reduced by these oscillations, was 34.6dBHz, i.e. 7.6dB below that for the data set shown in Figure 12. The frequency domain representation of the correlation data shows that the oscillation has a fundamental frequency of 81Hz. For this data set the blade passing frequency is:

$$\frac{0.745*1609*4}{60} = 79.9\text{Hz}$$

Clearly the fundamental frequency of the oscillation in the correlation data is again very similar to the blade passing frequency. Further evidence of the correlation between the frequency of the oscillations in the correlation data and the rotor speed are presented in Section 5.5.

This analysis of the snapshot data gathered for signals received through the tail rotor has confirmed that the ISN receiver did indeed suffer some form of signal 'interference' when the rotors were turning. This 'interference' acted in such a way that the received signal power was reduced for a percentage of the time, the percentage being dependent on the rotor speed, and most likely the mark-space ratio for the given signal pierce point on the rotor disc. The reduction in received signal power will, of course, lead to a reduction in the received CNR.

5.4 Snapshot data with rotors turning - main rotor

Tests were performed to investigate if the observed 'interference' caused by rotation of the tail rotor is also produced by the main rotor. The common antenna used by the receivers during the trial was switched from that on the tail fin to that on the nose of the aircraft. Snapshot data was then gathered for a number of different scenarios. Figure 18 gives the correlation totals for PRN 14 during a period when the rotors were turning at a recorded speed of 105.8% Nr. The satellite was at an elevation angle of approximately 45°, and a relative azimuth of approximately 330° at this time.

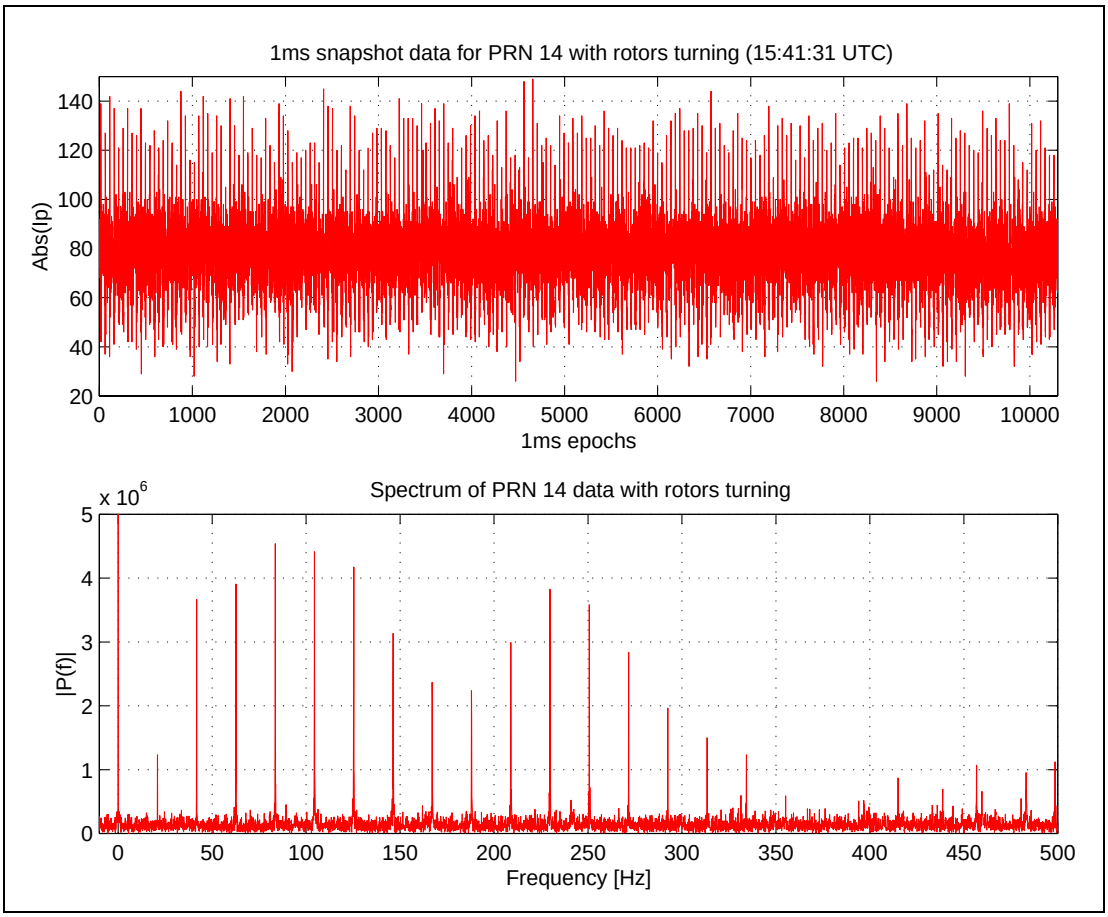

Figure 18 Snapshot data and frequency representation for PRN 14 with rotors turning

The I_p correlation totals are clearly being affected during this period of time, with a significantly increased variance in comparison to the data sets, shown previously in Section 5.2, when the rotors were stationary. It can be seen that there are again oscillations in the data. However, it is important to note that as well as there being oscillations that cause reductions in the signal level, there are also those that cause increases in the signal level. Consequently, this large number of oscillations leads to there being many large components in the frequency domain representation of the received signal envelope data, as shown in the lower plot. The first significant frequency component is at 20.9Hz; the remaining components are harmonics of this frequency. However, it is important to note that the signal at the fundamental frequency (20.9Hz) is not the dominant signal, as was the case with the tail rotor data. This suggests that there are multiple effects occurring as each main rotor blade passes between the incoming signal wavefront and the antenna. The estimated blade passing frequency for this data set is 20.7Hz. Hence the 'interference' effect observed in the correlation data gathered on the main rotor is also clearly a function of the rotor speed, or more specifically, the blade passing frequency.

The complex nature of the correlation data for this data set is shown in Figure 19 where a more detailed examination of the profile is presented. As the estimated blade passing frequency is 20.7Hz, the period between rotor blades is 48.4ms. For this particular satellite at the elevation and azimuth at which the signal pierces the main rotor disc, the percentage of time that the rotor blade will 'block' the signal path is very small (approximately 5%). Both effects can clearly be seen in this data set. When the blades 'block' the signal path there is first a fast reduction in the signal level followed by a very large increase. This is subsequently followed by a reduction before the signal level returns to normal. The increase in signal level is very large indeed. When considering the received power profile ($I_p^2+Q_p^2$) these increases are typically in excess of 100% of the power when the rotor blades are not 'blocking' the signal. This effect was also observed for the same satellite when the rotor was turning at a speed of approximately 70% Nr.

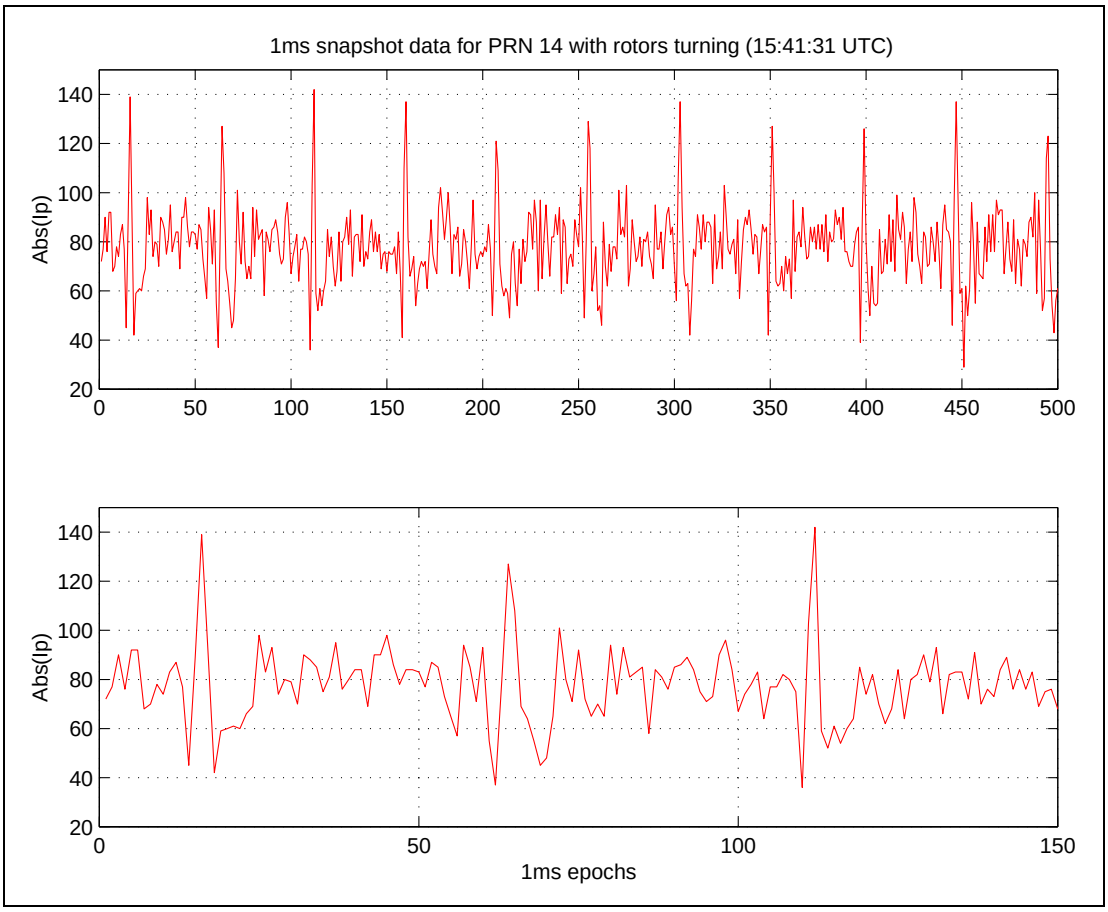

Figure 19 Close up of PRN 14 data for main rotor

This analysis of the snapshot data gathered for signals received through the main rotor disc has confirmed that, as was the case for the tail rotors, signal perturbations are produced when the rotors are turning. The nature of the observed perturbations was clearly different from those observed for the tail rotor. Further investigations would be required to determine if this is due to the specific satellite-rotor-antenna geometries concerned in the data sets processed, or if it may be due to physical differences such as different blade constructions for the tail and main rotors. However, for the purpose of this investigation it has been shown that signals received through both the tail and main rotor discs are subject to perturbations when the rotors are turning.

5.5 Correlation between rotor speed and observed oscillations

In this section the correlation between the blade passing frequency and the frequency of the oscillations produced in the correlation data is examined. This is performed on tail rotor data for a number of start/stop and stop/start sequences.

The first data set to be shown is that during a reduction in rotor speed from full speed. The satellite being tracked was PRN 30 which was at an approximate elevation angle of 24^o and a relative azimuth of 270^o. For the 10 seconds of snapshot data 10 individual 1 second data sets were formed, allowing the frequency of the oscillations in the snapshot data to be determined during this time period. The frequency is established by identifying the largest component in the frequency domain representation of the received signal envelope, P(f), excluding that at DC. The resolution of each of the 10 frequency estimates is 1Hz. The frequency of the oscillations produced in the $I_p^2+Q_p^2$ data is shown in Figure 20. The blade passing frequency is also shown, which has been calculated from the recorded rotor speed data.

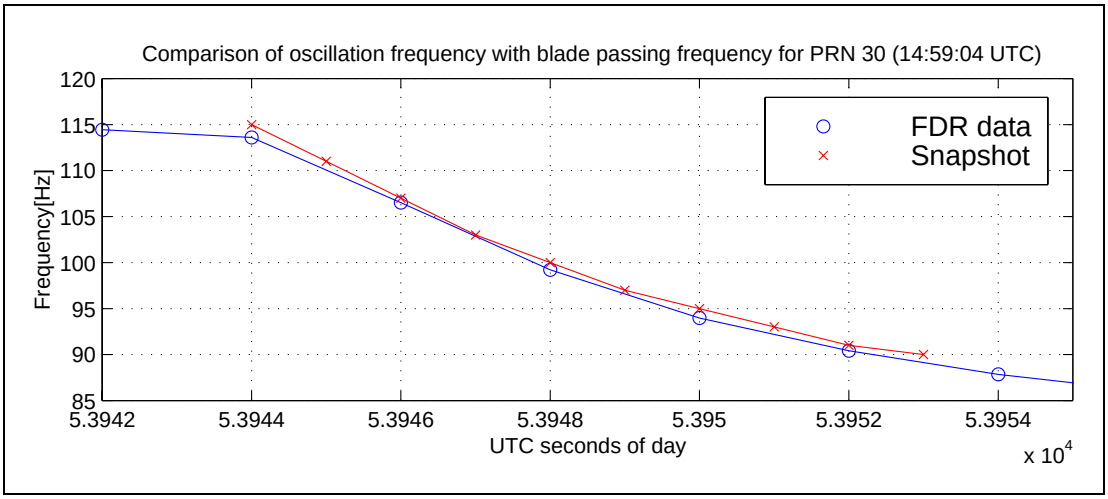

Figure 20 Comparison of oscillation frequency with blade passing frequency for PRN 30

The oscillation frequencies clearly reduce in a very similar manner to the blade passing frequency. Given the accuracy of the recorded rotor speed, together with the resolution of the oscillation frequency estimates, it is reasonable to conclude that the passage of the tail rotor blades between the antenna and the incoming signal is in some manner causing the perturbations in the received signal. Further evidence will now be shown.

Figure 21 presents a comparison of the oscillation frequency with the blade passing frequency for PRN 28, during a period when the rotor speed was increasing to full speed. Again, it is clear that the oscillation frequency is essentially the same as the blade passing frequency. As the oscillation frequency and the blade passing frequency reach steady state values, it is clear that the oscillation frequency is slightly the larger of the two. This is consistent with the results obtained when the rotors were at full speed during steady state conditions. No significance is, however, attached to the difference since its magnitude is within the bounds of the stated measurement accuracy.

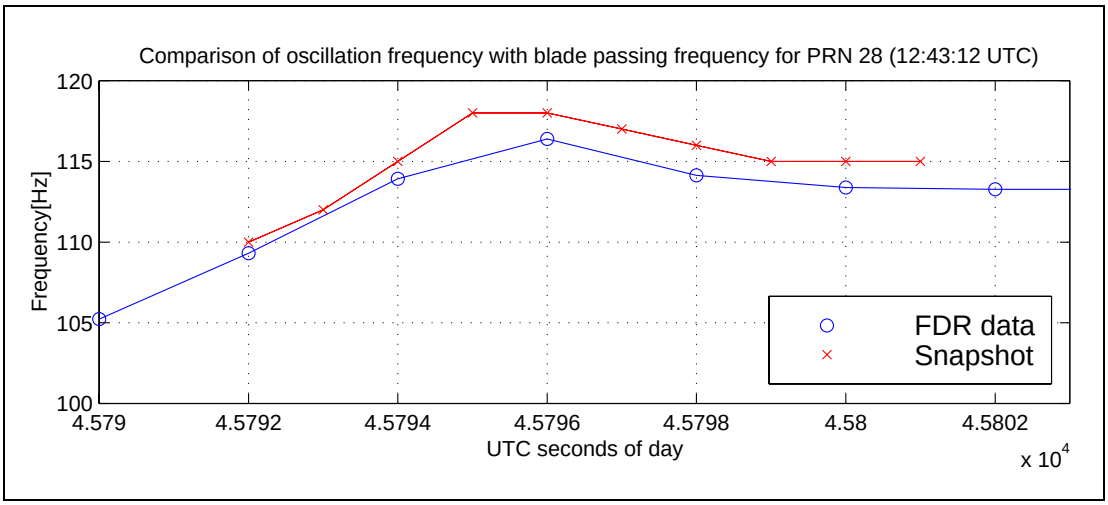

Figure 21 Comparison of oscillation frequency with blade passing frequency for PRN 28

The final data set to be presented in this section is again from PRN 30. The rotor speed is increasing during a start-up sequence. As can be seen in Figure 22, there is a very strong correlation between the oscillation frequency and the blade passing frequency.

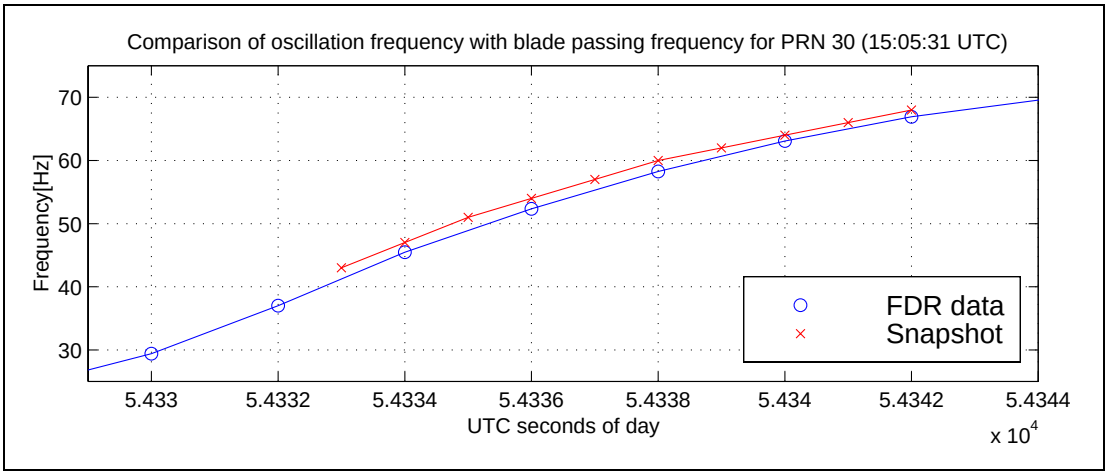

Figure 22 Comparison of oscillation frequency with blade passing frequency for PRN 30

It is suggested that the data presented in Figure 20, Figure 21, and Figure 22 represents compelling evidence of the correlation between the blade passing frequency and the frequency of the oscillations produced in the correlation data.

5.6 Estimation of attenuation caused by rotors

Having determined that both the tail and main rotor blades cause some form of attenuation of those GPS signals received through either of the rotor discs, it is important to attempt to estimate the attenuation induced. Combining this estimate with the knowledge of the blade passing frequency and the percentage of time the blades 'block' a particular signal path to the antenna, it is possible to characterise the signal that would be received at the antenna. In this section a relatively simple technique to estimate the attenuation caused by the rotor blades is presented, and the resulting estimated attenuation values are given. This estimation has been performed solely for the tail rotor blades as there was insufficient snapshot data recorded for the main rotor blades to provide a meaningful set of results.

In Section 5.2 it was shown that when the rotors are stationary the I_p correlation totals (with navigation data removed) are essentially fixed at a constant level, over a short time period, with the variance about this level dependent on the CNR. As was shown in Section 5.3, when the rotors are turning the correlation totals reduce from the constant level as each blade passes the signal pierce point. The level to which the correlation totals drop appears also to be a constant level. Again the correlator totals will have a variance about this level also. Estimating both levels would allow the attenuation induced by the rotors to be estimated. Estimation of these two levels is, however, made difficult by the noise level on the correlation data.

A simple method of estimating these two levels is to define a threshold value in order to separate the data into the two categories; those deemed to be when the signal is received without attenuation and those when the signal is attenuated. Having defined which correlation totals are in each category the mean of each category will be the best estimate of the two levels that represent the partitioned data. These two mean values shall be referred to as Hi and Lo. Therefore a two-level model of the data can be produced. Those correlation values above the threshold can be represented using the value of Hi and those below (or equal to) the threshold can be represented using the value of Lo. However, the choice of threshold value will have a significant effect on the results obtained. The optimal choice of threshold will be that which minimises the differences between the actual correlation data and the two-level model of that data. Therefore the optimal threshold is defined to be that which minimise the sum of the squares of the residuals, where the residuals are the differences between the model and the actual data. Having obtained the optimal values of Hi and Lo the attenuation induced by the rotor blades can then be calculated. The steps involved in forming these estimated attenuation values can be summarised as follows:

a) Form correlation data quantity $I_p^2+Q_p^2$.

b) Define the threshold.

c) Calculate value of Hi by forming the mean of those correlation data totals above the threshold value.

d) Calculate value of Lo by forming the mean of those correlation data totals below or equal to the threshold value.

e) Form a new data set the same length as the correlation data set.

f) For all those samples in the original correlation data set that were above the threshold value assign the corresponding element in the new data set a value of Hi.

g) For all those samples in the original correlation data set that were below or equal to the threshold value assign the corresponding element in the new data set a value of Lo.

h) Difference the new data set with the original correlation data to form the residuals.

i) Calculate the sum of the squares of the residuals.

j) Determine the threshold value that minimises the sum of the square of the residuals.

To more clearly demonstrate this estimation technique a comparison of the two-level model produced for one of the PRN 28 snapshot data sets is presented. The data is taken from a period when the rotors were almost at full speed (105.9% Nr), at 12:57:50 UTC. This rotor speed corresponds to a blade passing frequency of 113.6Hz. The satellite was at an elevation angle of approximately 38^o and a relative azimuth of 270^o. The optimal threshold value for partitioning the $I_p^2+Q_p^2$ data was found to be approximately 4460, resulting in an estimated attenuation value of 4.94dB. The two-

level model data that is produced for this threshold value is shown in Figure 23, where it is compared to the raw correlation data.

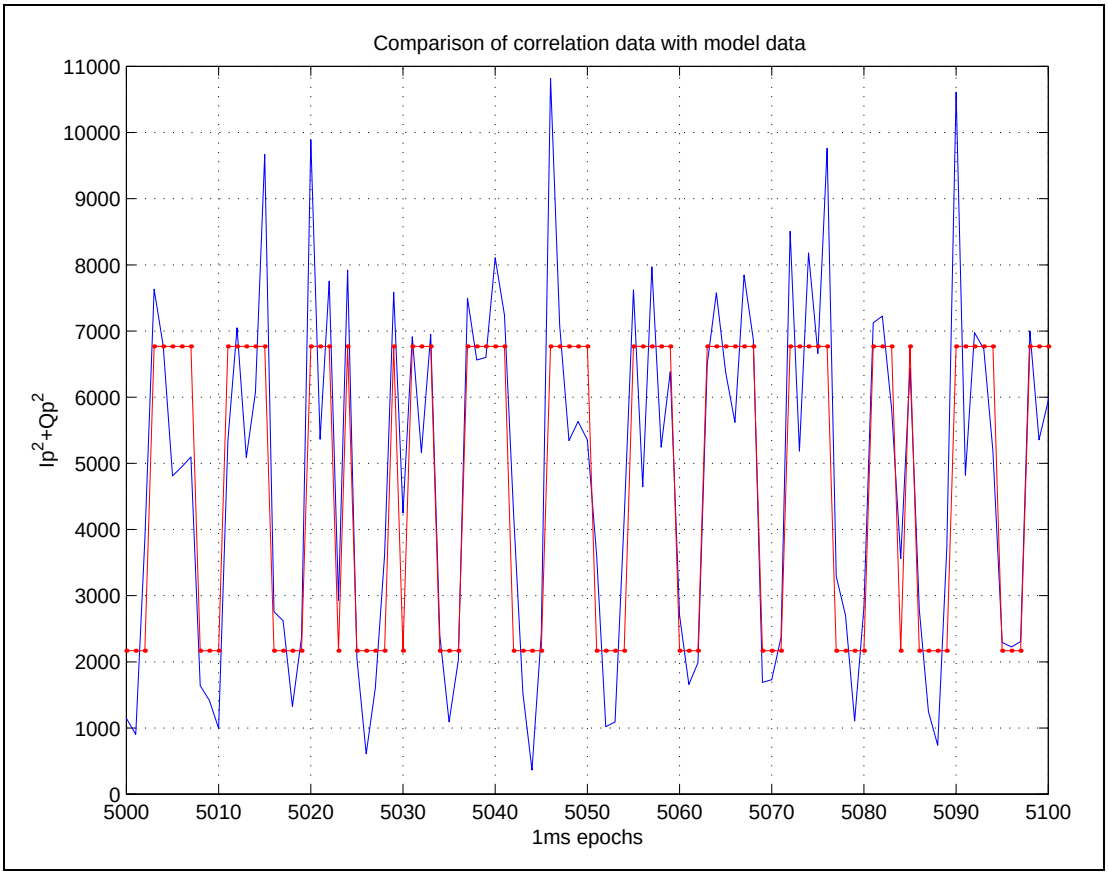

Figure 23 Comparison of PRN 28 correlation data with two-level model

The two-level model provides what can best be described as a reasonable fit to the correlation data. Although the Hi and Lo values shown do not immediately appear to be the optimal levels for the segment of data shown, they are the values that minimise the sum of the squares of the residuals over the entire data set, which is 10,300 epochs in length. It is clear that this simple model will have severe limitations when presented with more complex data, for example, the multiple oscillations produced on the main rotor snapshot data presented in Section 5.4. The results of this modelling technique are now presented for the snapshot data sets captured during the trials. The results presented are for the snapshots captured on the tail antenna as the complex oscillations produced on the main rotor can not be accurately modelled using this simple technique.

The first results presented are those for PRN 28. The data sets processed were between 12:57:31 UTC and 13:25:00 UTC. During this time the satellite moved from an approximate elevation of 38^{o} and relative azimuth of 265^{o} to an elevation angle of 28^{o} and a relative azimuth of 270^{o}. A total of 13 data sets were taken for this satellite, of which 12 were when the rotors were at full speed and the remainder at approximately 90% Nr. Each data set lasted for 10.3 seconds as the data captured consisted of 1ms correlation totals. The estimated attenuation values are shown in Figure 24, where the estimate made when the rotor speed was 90% Nr forms the

last data point. The mean of these estimates is 5.22dB, which is close to the value predicted previously when inspecting the profile given in Figure 14.

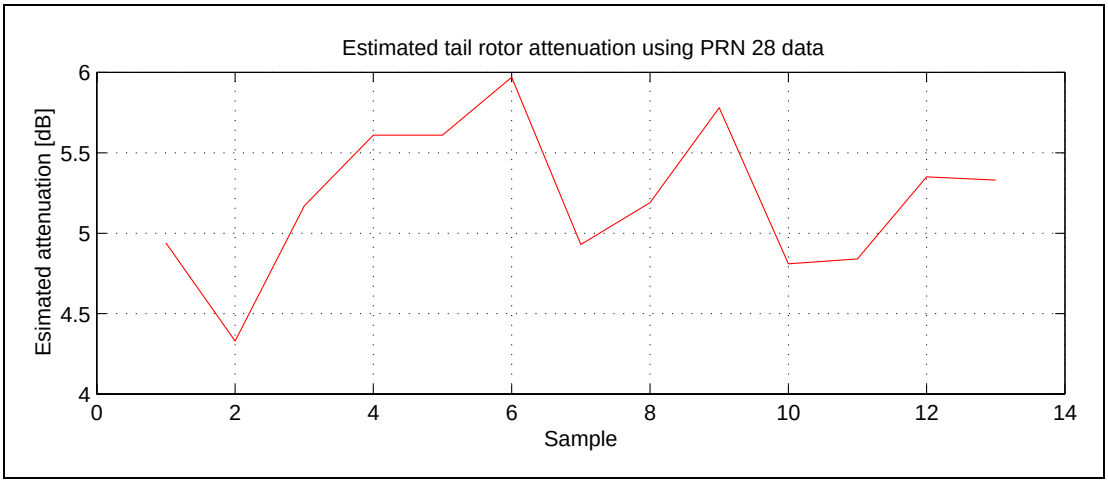

Figure 24 Estimated tail rotor attenuation using PRN 28 data

The estimated attenuation level obtained from the snapshot data gathered for PRN 30 is now presented. The PRN 30 data was gathered between 14:55:29 UTC and 15:23:46 UTC. At the beginning of this period the satellite was at an approximate elevation angle of 24^{o} and a relative azimuth of 270^{o}. At the end of this period the approximate elevation angle was 36^{o} and the relative azimuth was 265^{o}. In total 26 snapshots were captured during this time. The majority of these were with the rotors turning at full speed, although others were captured during times when the rotor speed was changing, i.e. a start-up or shutdown procedure. The estimated attenuation for these snapshots is shown in Figure 25. The mean of these estimates is 3.82dB.

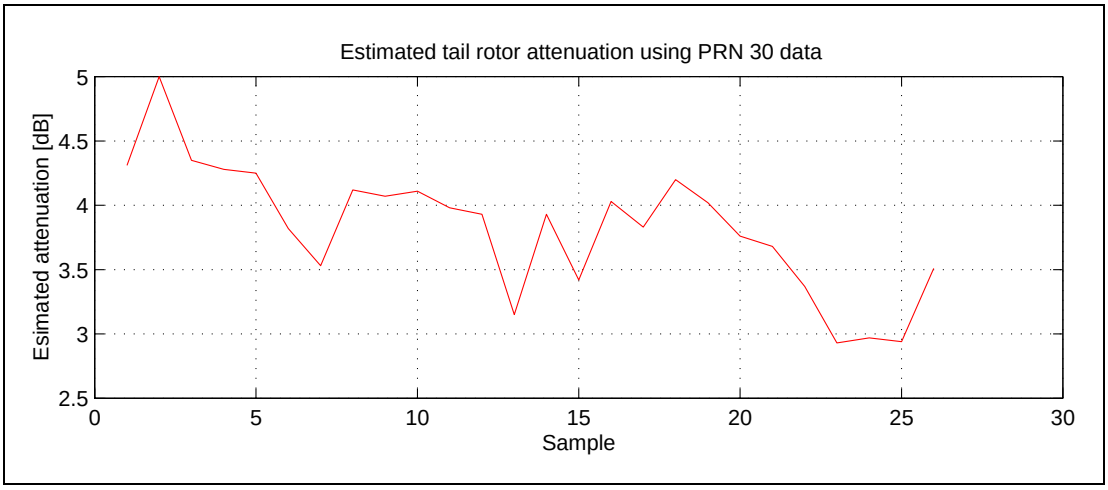

Figure 25 Estimated tail rotor attenuation using PRN 30 data

Given knowledge of the attenuation induced by the rotor blades, together with the percentage of time a given signal is 'blocked' by the rotors it is possible to predict the nature of the overall signal that will be seen at the receiver. As has been shown, given the noisy nature of the correlation data obtained during these trials, it is difficult to accurately estimate the attenuation of the rotor blades. There is a relatively large difference in the attenuation estimates produced when using the snapshot data for PRN 28 and when using that for PRN 30. However, it must be remembered that the estimation technique uses a very simple model of the perturbation in the correlation data. In order to better estimate the attenuation levels induced by the rotor blades it would be necessary to develop a data model that is more accurately based on the

construction of the rotor blades themselves, which is beyond the scope of this study. The attenuation estimates produced in this section serve to indicate the magnitude of the effect on the aircraft being used.

5.7 Multipath effect observed with tail rotor

Whilst analysing the snapshot data obtained on the tail rotor an unexpected result was obtained. The satellite for which snapshot data was obtained was one whose signal reached the antenna directly, i.e. without passing through the rotor disc. This satellite was being tracked during the trial in order to obtain control data, showing the 'normal' behaviour of signals not propagating through the rotor disc. The correlation data for this satellite, PRN 4, is shown in Figure 26 over a 200ms period. The satellite was at an elevation angle of approximately 24^{o} and a relative azimuth of approximately 90^{o}. The recorded rotor speed at this time was 105.9% Nr, corresponding to a blade passing frequency of 113.6Hz. There are clear oscillations in the Ip data that are similar to those shown previously in Section 5.3. Inspection of the frequency domain representation of this data set reveals that the oscillation is at a frequency of 115Hz, which is again essentially the blade passing frequency, given the accuracy of the recorded rotor speed. Therefore, even though the signal is not propagating through the tail rotor disc, the tail rotor is still having an effect on the received signal. It should also be noted that there is a significant frequency component at 57.5Hz for this data set, although it is not as large as that at 115Hz. This can clearly be seen in the data set as an oscillatory effect with a period in the region of 17.4ms. The implication is that there is some component of the tail rotor assembly which is providing a contribution to the modulation with a period corresponding to alternate blade passages.

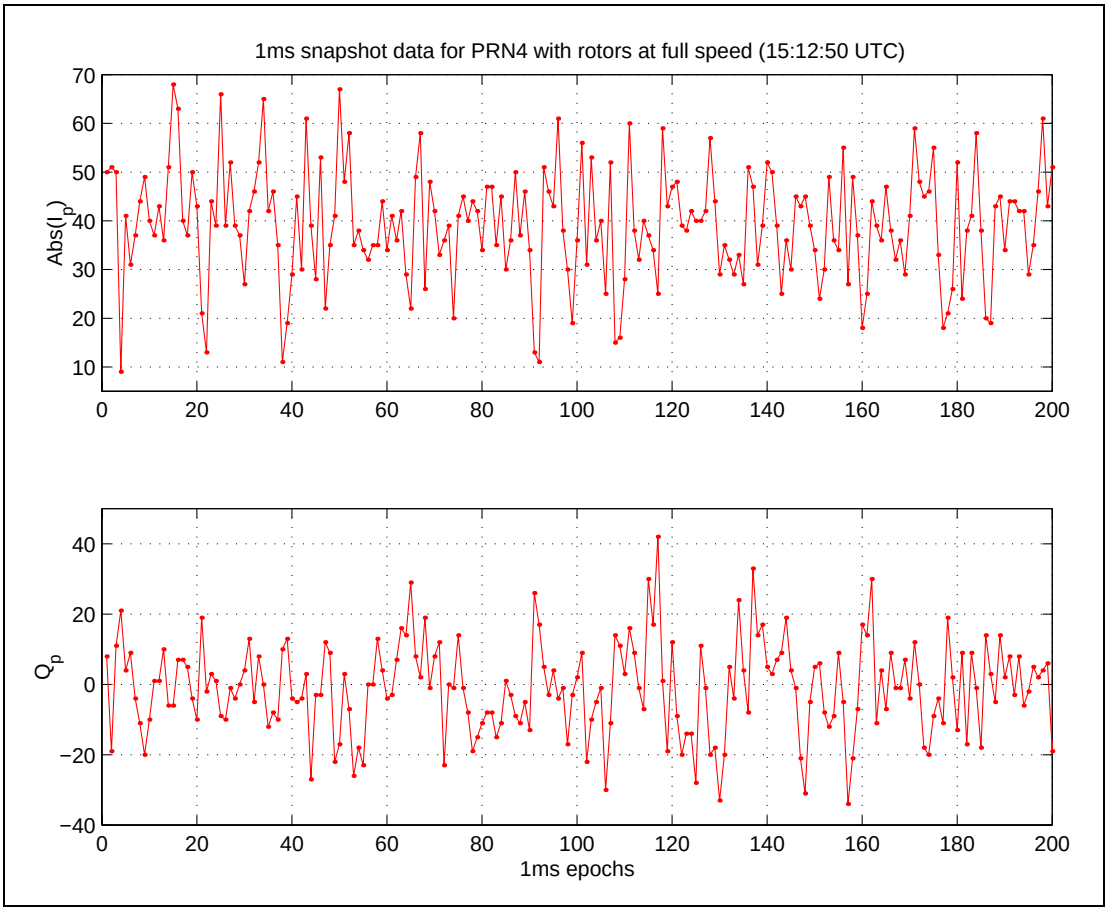

Figure 26 1ms snapshot data for PRN 4 with rotors at full speed

The most likely explanation for the 115Hz oscillation in the correlation data is that the rotors are causing a multipath signal to be produced that affects the received signal amplitude. According to the geometry of the satellite with respect to the antenna and tail rotor disc, this multipath signal will only be produced when a rotor blade is in the appropriate position. Hence, as the rotors turn the multipath signal will appear and disappear, as is seen in the correlation data. If this is indeed the mechanism that is causing the 115Hz oscillation in the PRN 4 correlation data, then it appears that the multipath signal is causing destructive 'interference' in this case. However it should be noted that, depending on the geometry concerned, it is equally likely that at other elevations and azimuths the multipath produced could be constructive. Unfortunately no other snapshot data was gathered during the trials for satellites not being received through the rotor disc. Therefore it is not possible to determine the range of elevations and azimuths over which this effect occurs.

6 Effect of Rotors on Range Measurement Precision

6.1 Introduction

It has been shown in Section 5 that rotation of the tail and main rotors causes perturbations in the received signal. For the tail rotor, and to a lesser extent the main rotor also, these perturbations were seen to cause the received signal power to be reduced each time the blade passed between the antenna and the incoming signal wavefront. Consequently the average received signal power is reduced by these perturbations. Both code and carrier phase measurement precision are inversely proportional to received signal power. An increase in the measurement noise will lead to an increase in the receiver's position fixing error. Hence there are potential operational impacts that could be caused by the effect of the rotors on the received GPS signals. This section will therefore investigate whether the reductions observed in the average received signal power during the trials performed had any impact on the range measurement precision.

6.2 Tail rotor

The range measurement data that has been analysed in this section is that from the Navstar receiver only. The reasons for this are as follows:

- Code and carrier phase observables were not accessible from the Trimble receiver.
- To analyse the range precision requires significant periods during which code and carrier phase observables were consistently produced by the receiver, with no carrier cycle slips. The ISN receiver could not provide the required periods of such data due to the need to stop and start the receiver in order to save the snapshot data.
- The Navstar receiver provided continuous code and carrier phase data for long periods of time.

The Navstar receiver is an L1 GPS C/A code receiver which provides the following output observables; pseudorange, accumulated delta range (ADR) and Doppler. As its name suggests, the ADR measurement is formed by accumulating the high precision, but ambiguous, carrier phase measurements. Each carrier phase measurement is in fact a differential range measurement over the measurement period. Hence the ADR is a biased range measurement, with the bias being the integer carrier cycle ambiguity at the time of the first measurement. Using the pseudorange and ADR data it is possible to assess the pseudorange accuracy. The measured pseudorange and ADR can be expressed as follows:

$$\rho = R + \frac{I}{f^2} + T_{rx} + \eta_{code} + Trop + M_{code} + T_{sv} + \varepsilon$$

$$\phi = R - \frac{I}{f^2} + N\lambda + T_{rx} + \eta_{carr} + Trop + M_{carr} + T_{sv} + \varepsilon$$

where,

ρ is the measured pseudorange, in metres

ϕ is the carrier phase derived ADR, in metres

R is the satellite-user range, in metres

I/f^2 is the frequency dependent ionospheric delay, in metres

T_{rx} is the receiver clock offset from system time, in metres

η_{code} is the code tracking noise, in metres

η_{carr} is the carrier tracking noise, in metres

$Trop$ is the tropospheric delay, in metres

M_{code} is the code multipath error, in metres

M_{carr} is the carrier multipath error, in metres

T_{sv} is the satellite clock offset from system time, in metres

ε is the satellite ephemeris position error, in metres

f is the carrier frequency, in Hertz

N is the integer carrier cycle ambiguity

λ is the carrier wavelength, in metres

Differencing the pseudorange and ADR, many of these terms cancel:

$$\rho - \phi = 2\frac{I}{f^2} + \eta_{code} + M_{code} - N\lambda - \eta_{carr} - M_{carr}$$

Given that the carrier multipath error and the carrier tracking noise are an order of magnitude smaller than the corresponding code multipath and code noise tracking contributions, they can be discarded. Provided there are no carrier cycle slips, the carrier integer ambiguity will remain fixed and so will simply form a bias. Hence the pseudorange minus ADR measurement provides an indication of the variance of the pseudorange; i.e. the multipath and thermal noise contributions. However, care must be taken when making such assessments as the ionospheric delay term remains within this expression. Generally the ionospheric delay will be slowly varying, hence it can be removed with a simple quadratic fit. The pseudorange minus ADR residual has therefore been used to determine the effect of the rotor blades on the pseudorange measurement noise.

The first data set to be presented is that from the Navstar receiver for PRN 28 between 11:48:09 and 12:35:11 UTC. This particular period was chosen as there was continuous carrier phase tracking throughout this time. The satellite began this period at an elevation angle of approximately 51^{o} and a relative azimuth of approximately 310^{o}. Three rotor start/stop sequences were performed during the data set. Figure 27 gives the pseudorange minus ADR residual for this time, with the arbitrary mean

value removed for presentation. The recorded rotor speed at these times is also shown.

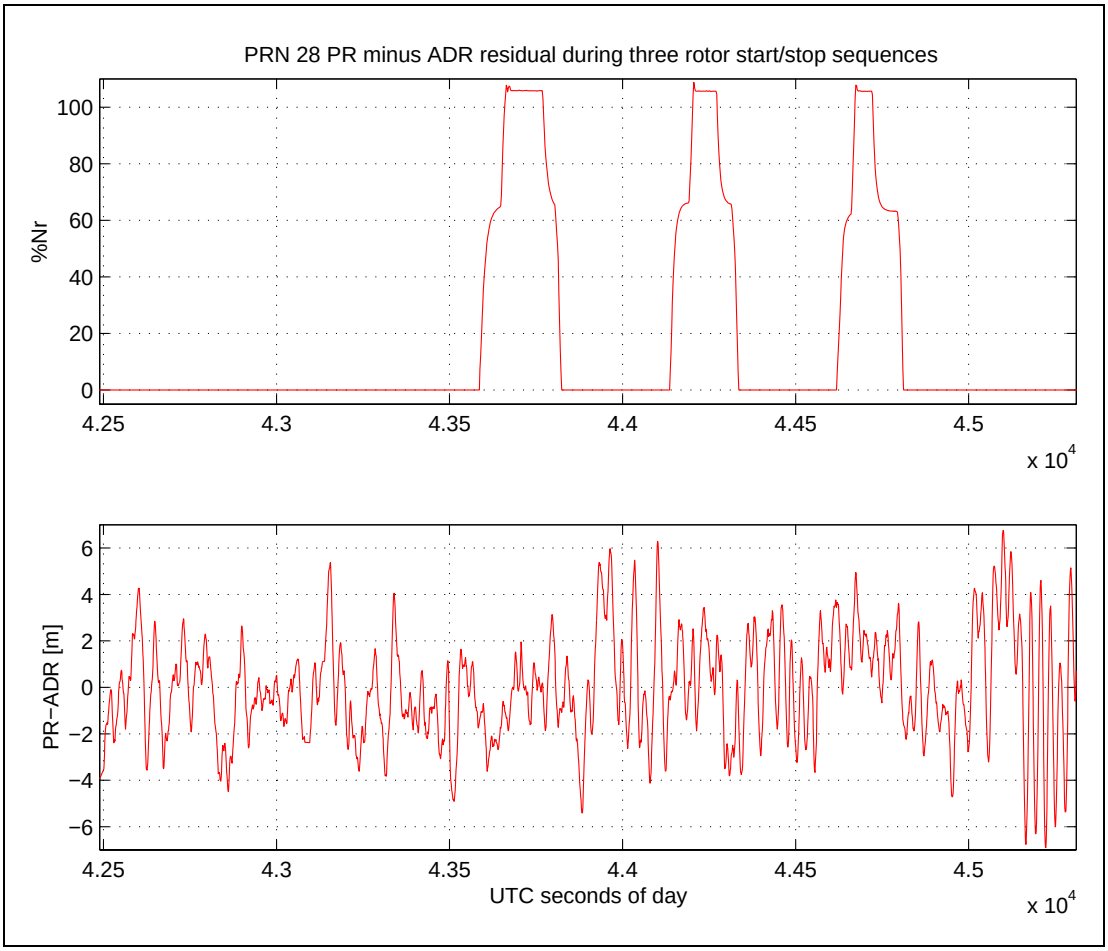

Figure 27 PRN 28 pseudorange minus ADR residuals for Navstar receiver

The pseudorange minus ADR residual is dominated by oscillatory structures, which are code multipath tracking errors. The code tracking noise can be seen to be the much smaller Gaussian noise on top of the structures. The receiver manages to successfully track through all three start/stop sequences in this time period. There is no obvious effect of these sequences on the pseudorange minus ADR residual. The range measurement precision does not, therefore, appear to have been increased significantly for these data sets. One possible reason for this could be that, for this data set, the code tracking noise is being masked by the large code multipath errors. Derivatives of the pseudorange minus ADR data were therefore formed in order to remove the deterministic multipath errors. Any increases in the code tracking noise will then be evident. The first and second derivatives of the data shown in Figure 27 are shown in Figure 28.

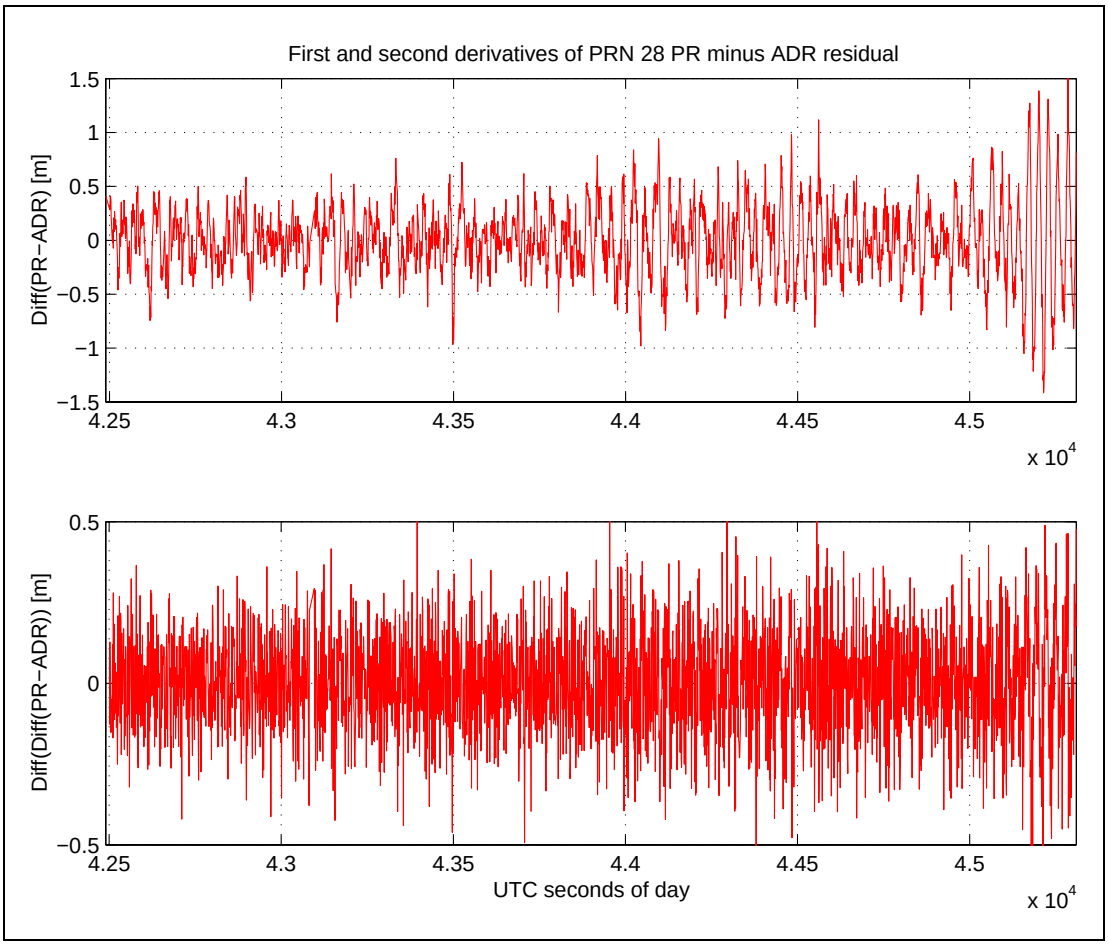

Figure 28 First and second derivatives of PRN 28 pseudorange minus ADR residuals

It can be seen that there are no discernible increases in code tracking noise when inspecting these derivatives. Therefore it has been found that, for this data set, the motion of the tail rotors does not cause any significant effects on the code tracking performance. Consequently the positioning performance of the receiver would not be adversely affected when processing such pseudorange data. However, further analysis of the pseudorange data is required before more definitive conclusions can be drawn.

Figure 29 gives the pseudorange minus ADR residuals for PRN 8 during the same three start/stop sequences shown in Figure 27. In this case the data set shown begins at 11:48:21 UTC and ends at 12:29:55 UTC, as this was a period during which the carrier phase data was continuous.

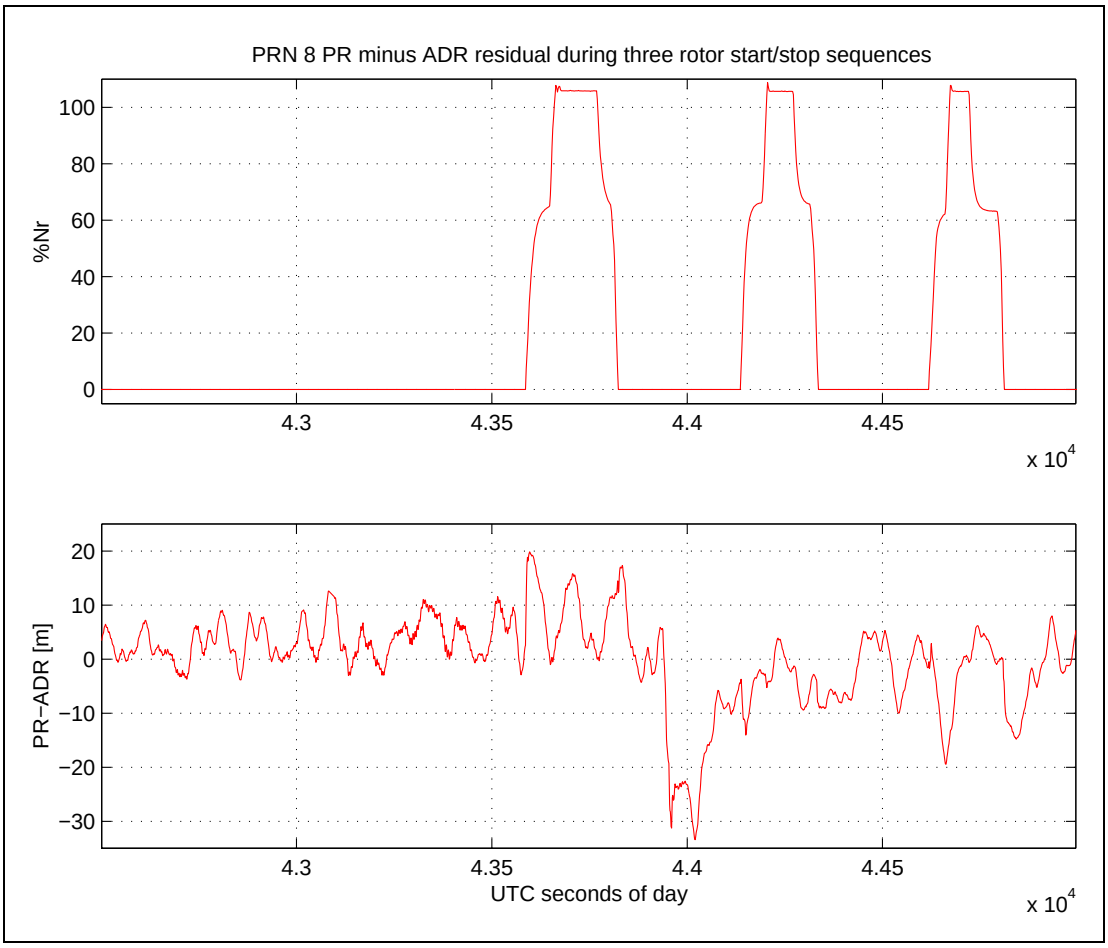

Figure 29 PRN 8 pseudorange minus ADR residuals for Navstar receiver

Again, the receiver is able to track this satellite through all three start/stop sequences. There is again no clear increase in code tracking noise, although the large code multipath errors may be masking such effects. The first and second derivatives of the residual data are given in Figure 30.

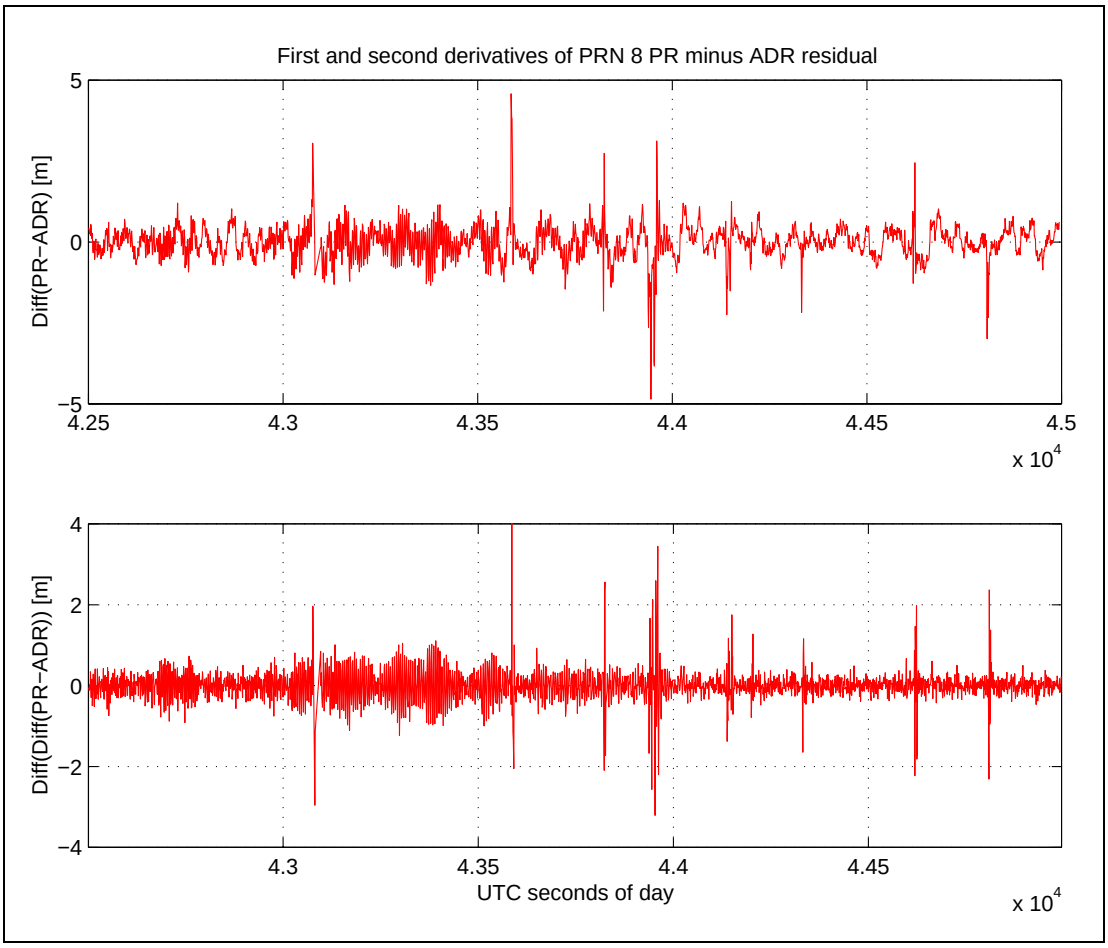

Figure 30 First and second derivatives of PRN 8 pseudorange minus ADR residuals

Therefore it can be concluded that for the tail rotor data sets processed there is no significant increase in code tracking noise caused by the reductions in the average received power. The turning of the rotors did, however, cause some tracking problems for the Navstar receiver when tracking PRN 8 for these three start/stop sequences. Figure 31 shows the receiver indicated channel status for PRN 8. A channel status of anything less than 5 indicates that the satellite is not being tracked properly. When the rotors are turning the tracking status is less than 5, indicating that the signal can not be tracked properly by the receiver. However, as the pseudorange minus ADR data is not producing large tracking errors during this time, it is most likely that the receiver is having problems with carrier tracking but not code tracking. It should be noted that there were no such tracking problems for the Navstar receiver when tracking PRN 28 through the same three start/stop sequences. This is most likely to be due to the increased signal strength of this satellite as it was being received at a higher elevation angle.

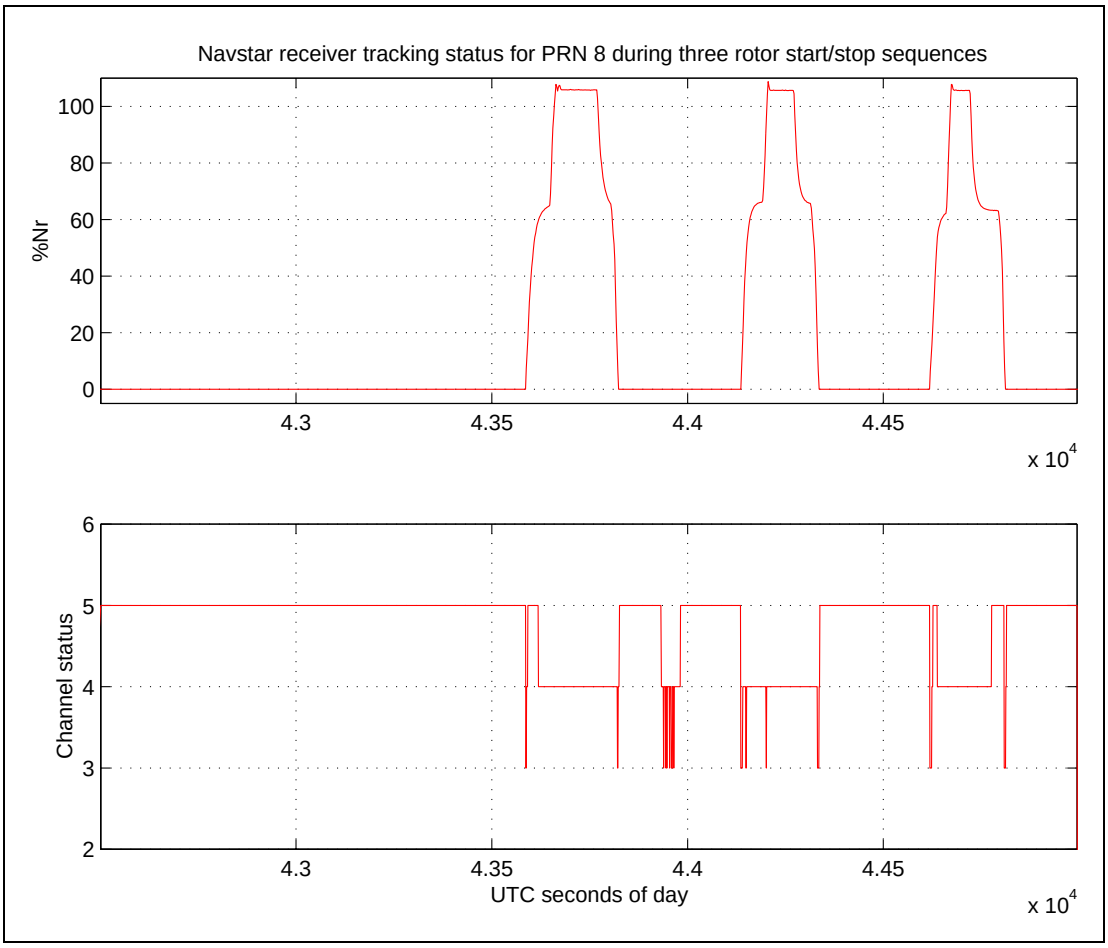

Figure 31 Navstar tracking status for PRN 8 during three rotor start/stop sequences

6.3 Main rotor

The effect of the main rotor on the range measurement precision is presented in this section. Figure 32 shows the pseudorange minus ADR residual for PRN 14 during a rotor start/stop sequence. The data set spans the interval 15:36:17 UTC to 15:46:30 UTC. During this time the satellite is at an elevation angle of approximately 47^{o} and a relative azimuth of 330^{o}.

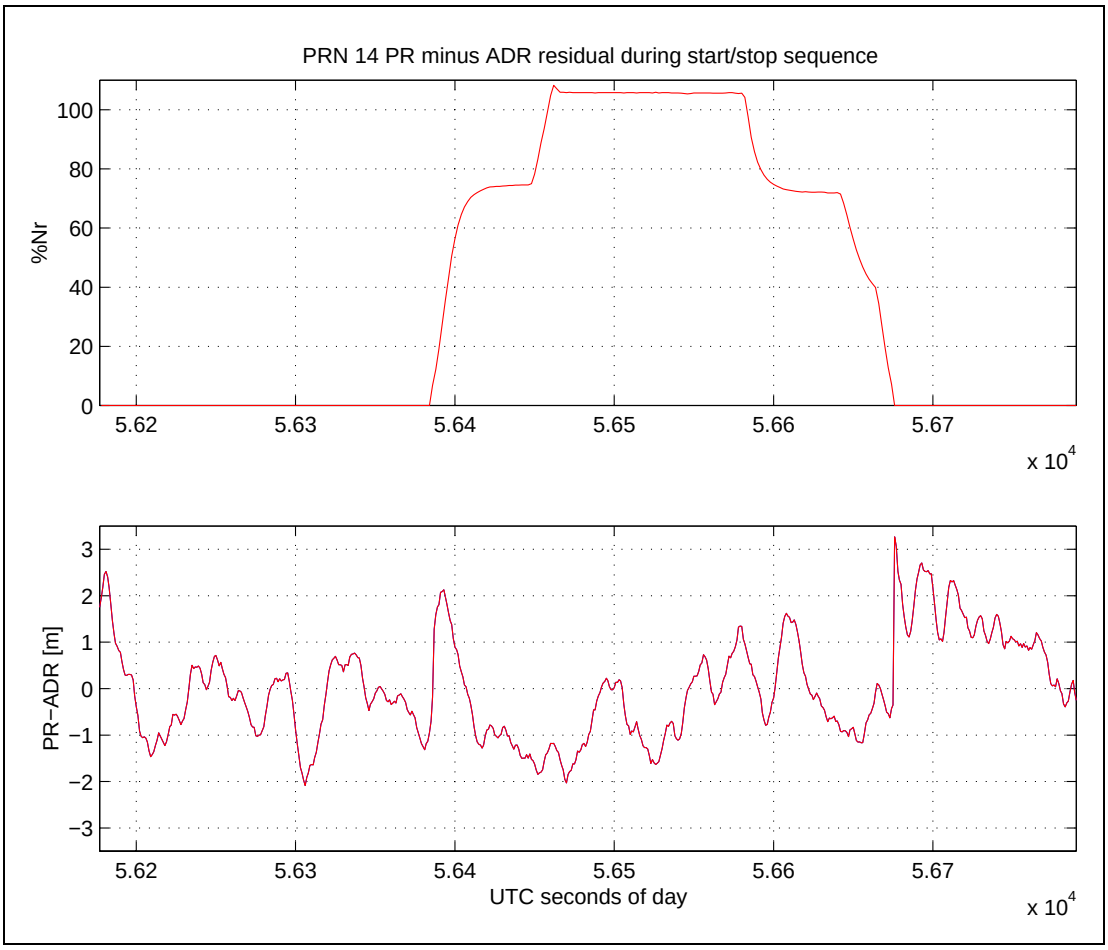

Figure 32 PRN 14 pseudorange minus ADR residuals for Navstar receiver

There is again no clear increase in the code tracking noise level when the rotors are in motion. The noise level is very low for this satellite, well below the level of the deterministic (i.e. non-random) perturbations in the residual, which appear to be code multipath errors. The first and second derivatives of the pseudorange minus ADR residuals for PRN 14 have been formed in order to provide a more detailed inspection of the range measurement precision, and are shown in Figure 33.

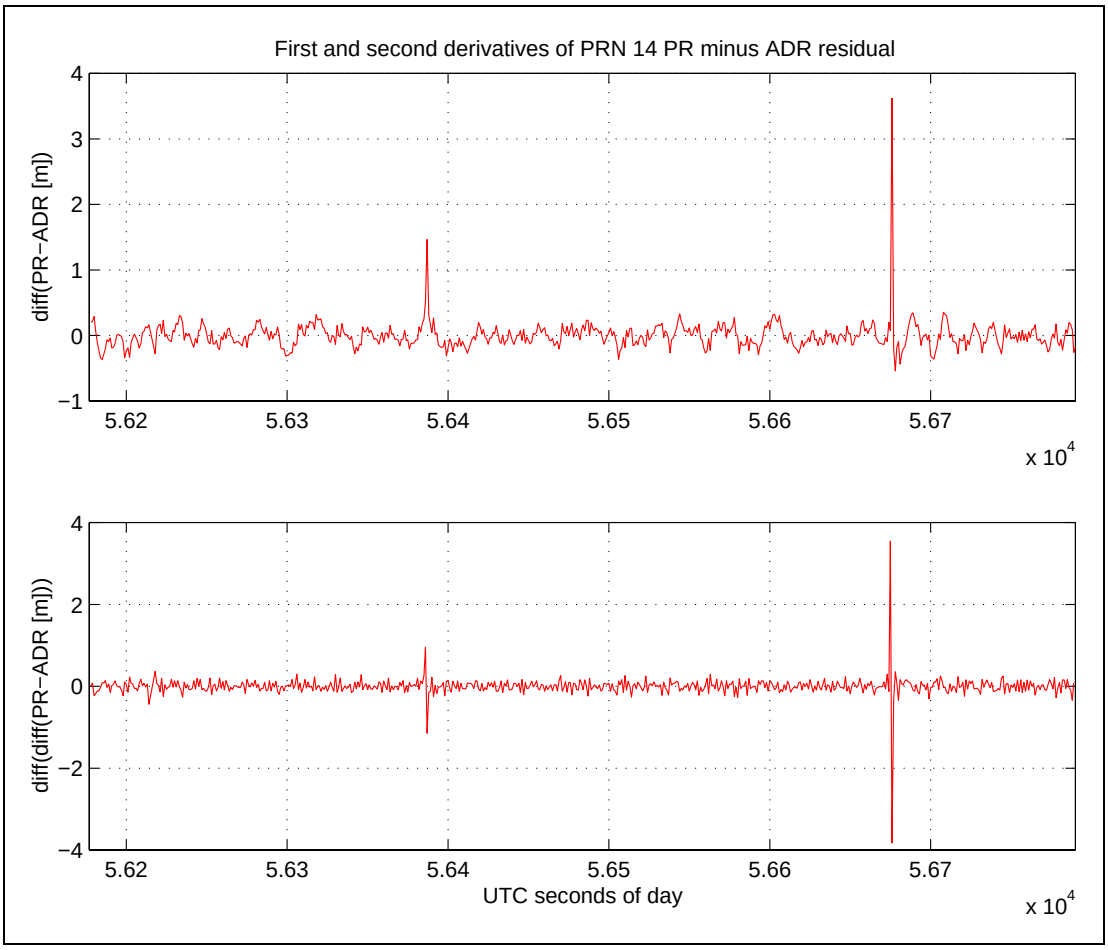

Figure 33 First and second derivatives of PRN 14 pseudorange minus ADR residuals

There is clearly no increase in the code tracking noise caused by rotation of the main rotors. However, there are two distinct spikes in the first and second derivative data, which relate to 'jumps' in the pseudorange minus ADR residual. These occur as the rotors are just beginning to turn and again as they are about to stop turning. Returning to the residual shown previously in Figure 32, these steps can be seen with careful inspection. As the residual is formed using both code and carrier phase data the 'jump' may be the result of either measurement changing. Analysis of the pseudorange data however reveals this to possess 'jumps' at the levels shown, confirming that it is the pseudorange measurement that is being affected. Therefore, whilst the turning of the rotors does not appear to have an effect on the range measurement precision, the starting and stopping of the rotors can cause 'jumps' in the pseudorange. Returning to the first and second derivatives shown in Figure 30 for PRN 8 for the three tail rotor start/stop sequences, it can be seen that 'jumps' also occur in those data sets as the rotors are starting and stopping. In that case the 'jumps' are a little less clear due to other unexplained spikes in the data. These 'jumps' show that the receiver has some difficulty in code tracking when the rotors are turning at very slow speed. Intuitively this is to be expected as the actual time the signal is blocked by each blade will be much greater at low speeds.

The first and second derivatives for PRN 9, during the same time period as was used for PRN 14 are shown in Figure 34. During this time the satellite was at an approximate elevation angle of 53^{o} and a relative azimuth of 167^{o}. Again, there is no identifiable increase in the range measurement noise. However, there are again clear spikes in the derivatives as the rotors start and stop.

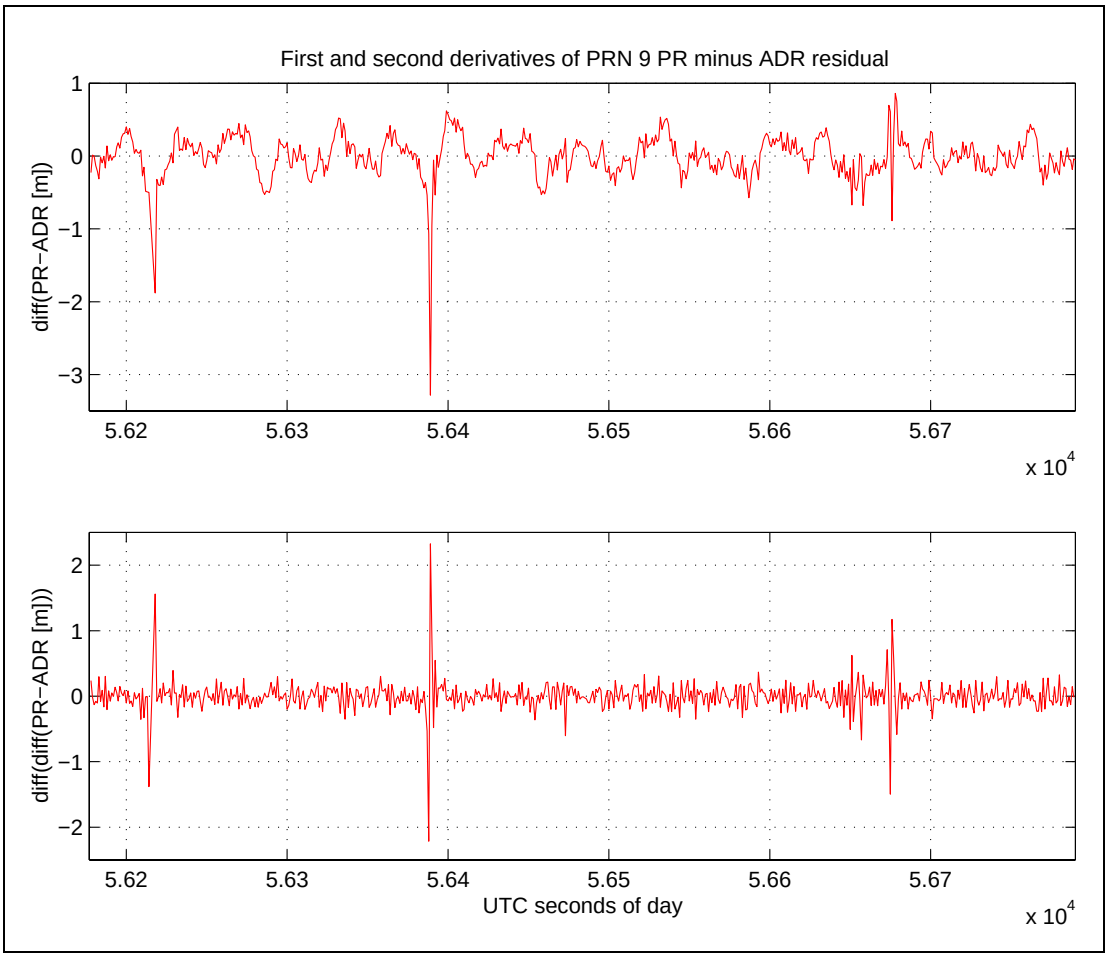

Figure 34 First and second derivatives of PRN 9 pseudorange minus ADR residuals

Hence it has been shown that for the data sets captured during the trial, rotation of both the tail and main rotors did not lead to a detectable increase in the range measurement noise. However, the starting and stopping of the rotors did cause small 'jumps' in the pseudorange measurements.

7 Effect of Rotors on Range Measurement Availability

7.1 Introduction

This section considers the impact of the rotor motion upon the ability of the two commercial GPS receivers (Navstar and Trimble) to perform range measurements upon a sufficient number of satellites to ensure the availability of a navigation solution. The analysis is based upon an examination of the real time tracking status flag associated with each receiver channel, which indicates whether the receiver is obtaining satisfactory 'lock' on the signal transmitted by the relevant satellite. Loss of lock on a particular channel implies that the receiver can no longer employ the associated PRN code observables (typically, pseudorange and delta-range) in the calculation of a navigation solution.

The number of such observables which are necessary to ensure 'availability' will vary according to the receiver architecture employed, for example the FD RAIM technique [2] requires five pseudorange measurements. The number of potential range measurements is not fixed; it will vary with time due to the motion of the satellite

constellation, and will also be affected by receiver design considerations such as the satellite elevation cut-off mask. All of these aspects are outside the scope of this study which is concerned solely with the changes in the availability of individual pseudorange measurements (specifically, any loss of tracking lock) between the rotors-stopped and rotors-turning states.

7.2 Tail rotor

A qualitative examination was first performed of the tracking status for the Navstar and Trimble receivers during the periods when the rotors were being turned slowly by hand. This revealed that, for the majority of the satellites, no instances of loss of lock were signalled by either receiver. The only exception was for a satellite (PRN 28) whose signal path to the tail mounted GPS antenna passed through the tail rotor disc close to the blade root: in this situation both receivers experienced a number of short breaks in tracking which could be correlated with the passage of a rotor blade. These interruptions did not occur on every blade pass: an isolated example affecting the Trimble receiver can be seen on the plot in Figure A.6 (page 57) at time 13:52:08.

The inference drawn from these results is that, with the rotors stopped, the position of the tail rotor blades had no impact upon the receivers' ability to track satellites where there was an unobstructed signal path to the antenna. However it was demonstrated that interposition of a blade between the satellite and the antenna could sometimes result in tracking being lost.

The tracking status was then examined for the rotor start/stop sequences. Data from one of these tests is shown in Figure 35 where the sold horizontal lines indicate the presence of valid range measurements for each PRN tracked by the receivers. The Navstar and Trimble architectures are different (for example the former is a twelve channel receiver, the latter an eight channel unit), and it is therefore not appropriate to perform a direct comparison between the two sets of results. In spite of these differences, it is apparent that losses of lock on several different satellites were experienced by both receivers during the rotors-running period.

Table 1 shows the positions of the satellites in the form of relative azimuth (measured clockwise from the aircraft nose) and elevation above the horizon. The table also indicates whether the signal path from the satellite to the antenna intersected the tail rotor disc.

Comparison with Figure 35 reveals that all of the satellites for which tracking problems were encountered were either all in positions intersecting the rotor disc, or else were at very low elevations.

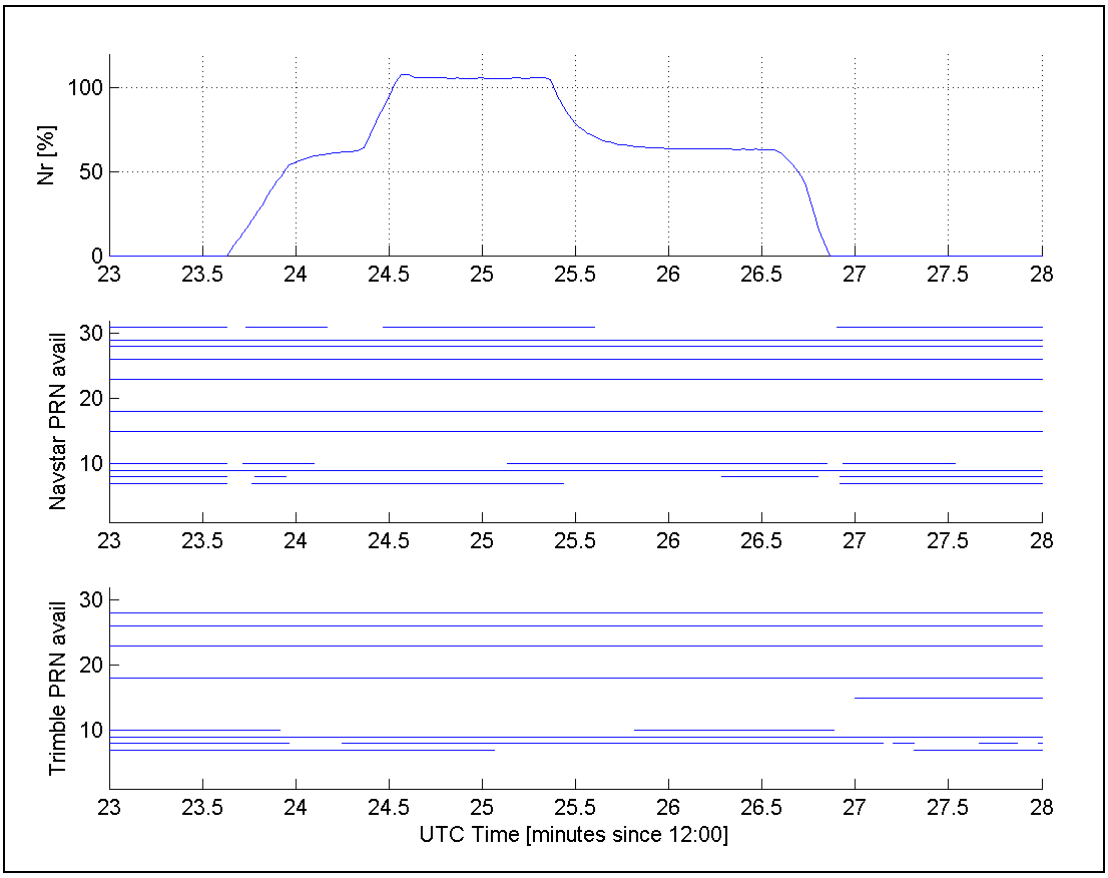

Figure 35 Range measurement availability during start/stop sequence - tail rotor

Table 1 Positions relative to aircraft for satellites in Figure 35

Satellite	Relative azimuth	Elevation	Intersects tail rotor?
PRN 7	330°	11°	Yes
PRN 8	286°	14°	Yes
PRN 9	104°	31°	No
PRN 10	032°	6°	No
PRN 15	137°	12°	No
PRN 18	158°	35°	No
PRN 23	066°	41°	No
PRN 26	019°	77°	No
PRN 28	285°	48°	Yes
PRN 29	001°	67°	No
PRN 31	220°	4°	No

A similar analysis was performed on the data from three other rotor start/stop tests and broadly consistent results were obtained. Once again, the satellites worst

affected by the loss of availability were all either in positions for which the signal path intersected the rotor disc, or were at very low elevations.

In an attempt to determine a statistical estimate for the magnitude of this problem, the percentage availability was computed for each of these tests for all satellites above an elevation mask of 10^{o}. In order to try to compensate for factors unrelated to rotor 'interference', such as constellation changes or the receiver's internal choice of satellites, data was only included in the analysis for those satellites which were being continuously tracked immediately before the rotors began to turn. The results are shown in Table 2.

Table 2 Range measurement availability statistics

Test number	Sample length [s]	Navstar range availability	Trimble range availability
1	238	87%	99%
2	198	84%	95%
3	192	86%	91%
4	213	95%	93%
All four tests	841	88%	95%

In [2], the concept of a "Realism Factor" was introduced, which represents the probability that a receiver provides a valid range measurement for a satellite which had been predicted to be available for tracking. Based upon in-flight data recorded using the Navstar receiver on the previous trials using G-SSSC, an estimate for the Realism Factor of 85.8% had been derived in that report by comparing the flight results with those derived from an offline simulation.

Although not directly compatible with the results in Table 2, which are based upon the difference between the rotors running and rotors stopped performance, it is of note that the previously computed Realism Factor is very similar to the overall range availability figure of 88% computed for the Navstar receiver. This would appear to add weight to the conclusion in [2] that the tail rotor "...is at least part of the cause of the low Realism Factor".

Although the corresponding range availability figure of 95% which was computed for the TSO-C129 compliant Trimble receiver is higher, suggesting that it is perhaps less susceptible to the rotor "interference" effect than the Navstar unit, it is clear from results such as those shown in Figure 35 that both designs of receiver are affected by the problem.

7.3 Main rotor

With the nose mounted antenna in use, the tracking performance of the two receivers was examined for the periods when the rotors were being turned slowly by hand. The relative geometry was such that there were five satellites in positions where the signal path intersected the main rotor disc at different points. No evidence was observed for any loss of tracking associated with passage of a rotor blade.

Figure 36 shows the tracking performance as a function of time for a start/stop test. It transpires that both receivers were tracking the same set of six satellites, all of which were positioned such that the signal path intersected the rotor disc (Figure A.14 in Appendix A). It can be seen that, with the exception of some short transient losses of lock at the very start and end of the rotor sequence (when Nr was less than

10%) affecting the Navstar receiver, rotation of the main rotor had no impact upon the availability of the range measurements.

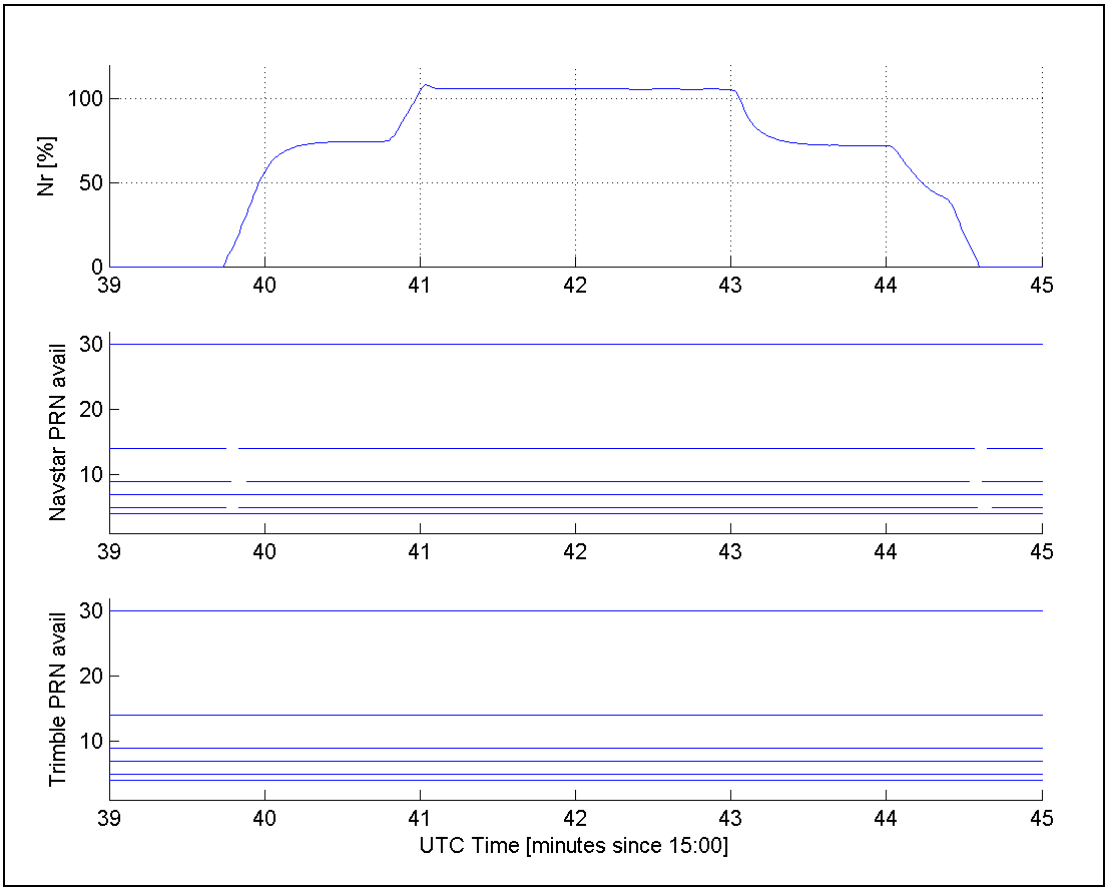

Figure 36 Range measurement availability during start/stop sequence - main rotor

In Section 6, it had been identified that 'jumps' in the Navstar receiver pseudorange errors for PRN 9 and PRN 14 occurred as the rotors started to turn and again as they came to a halt. Comparison with Figure 36 reveals that these events are correlated with a transient loss of lock on the satellites concerned and it is suspected that this is related to the extended blockage time caused by a blade rotating at very low speed.

Only a single start/stop sequence was performed involving the main rotor and therefore it was not possible to determine whether consistent results were obtained on multiple tests. Based upon this one test there is clearly no evidence for the rotor motion having caused a reduction in the availability of the range measurements (in contrast to the results which were obtained with the tail mounted antenna), with the exception of some short transient losses of lock at very low values of Nr.

8 Discussion

8.1 Rotor 'interference' characteristics

The purpose of the experiments described in this report was to provide a more detailed investigation of the effects which had been previously observed and which had been attributed to the rotor motion. Using the three dissimilar GPS receivers, and in particular the ISN unit with its high speed snapshot facility operating at the correlator level, it was possible to confirm that a rotor 'interference' effect was indeed present and that this (rather than, for example, an electrical interference source on the helicopter) had been the most likely explanation for the previous results.

Investigations into the effect of the rotor motion using the ISN equipment confirmed that the effect of rotor blade passage was to introduce perturbation, synchronised to the rotor rate, onto the received C/A code signals. These effects were observed irrespective of whether or not the signal path from the satellite intersected the rotor disc, although the effect was of a lesser magnitude when the signal did not intersect the disc.

The results suggest that the form of the modulation is more complex than a simple 'on:off' attenuation effect: in the case of the main rotor in particular, the oscillations included increases as well as decreases in the amplitude of the signal measured via the receiver correlators and contained significant spectral components at harmonics of the blade passing frequency. This suggests that both constructive and destructive RF 'interference' effects are at work during the course of each blade passage.

A comparison between recordings taken with the rotors running at differing rates reveals that the extent of the 'interference' effect did not exhibit any clear correlation with rotor speed, or with any speed-dependent parameter such as the blockage time associated with each blade passage. Estimates derived from the ISN snapshot data for the attenuation caused by the tail rotor blades were in the range 4dB to 6dB.

The results described above were obtained using two specific GPS antenna installations on a Sikorsky S76C helicopter and it cannot be assumed that these results would necessarily translate fully to other aircraft/antenna combinations: the scope of the trial did not allow an evaluation of such factors as the relative geometry between the antenna site and the rotors, or the construction of the rotor blades. However it is anticipated that the majority of rotary-wing GPS installations are likely to be affected by broadly similar modulation effects.

8.2 Impact upon navigation function

Having determined that a rotor 'interference' effect was present, attention then turned to its impact upon a receiver's navigation function. This was achieved by analysing the recorded data from commercial GPS receivers which were assumed to be sufficiently representative of typical operational equipment (one of these systems was a variant of a design certified to the TSO-C129 standard). The analysis was performed by considering, separately, the precision and availability of the pseudorange measurements which are employed by a receiver to compute its navigation solution.

Results obtained from an examination of the error characteristics of the range measurements generated by the Navstar receiver revealed no evidence to indicate a reduction in precision associated with the rotor motion, with the exception of some small 'jumps' in pseudorange when the rotors were turning very slowly (a situation which would not occur in flight). The implication of this result is that the impact of the rotors on range accuracy is negligible compared to the other error sources involved, and it supports the conclusion previously reached in [1] that the contribution of the

helicopter airframe and rotors to this receiver's navigation error was less than 2m. Unfortunately no pseudorange observables were available from the Trimble system and so it was not possible to repeat this analysis using a second commercial receiver.

An analysis of the range measurement availability (determined via the receivers' channel tracking flags) for the Navstar and Trimble systems, revealed clear evidence for a performance reduction correlated with rotor motion when the tail mounted antenna was in use. The effect was at its most severe in situations where the signal path from satellite to antenna intersected the tail rotor disc. Statistical analysis of the data yielded "Realism Factor" estimates of 88% and 95% for the Navstar and Trimble results, respectively.

Analysis of the corresponding data with the antenna placed beneath the main rotor revealed no evidence for any loss of availability, with the exception of transient effects at very low rotor speeds. Although this result would imply a "Realism Factor" approaching 100%, it is based upon very limited source data since only a single test was performed in this configuration.

The study did not consider any other aspects by which the rotor 'interference' might affect the performance of a GPS receiver. For example, it is conceivable that the rotor 'interference' could affect the ability of a receiver to decode the navigation data messages modulated onto the C/A code stream from each satellite. This may be of particular significance in SBAS systems where a similar data channel operating at a higher symbol rate is used to provide integrity information.

The conclusion from the available data is that rotor 'interference' is more likely to manifest itself as a loss of GPS availability rather than as a reduction in accuracy. Determination of the impact of the range availability results outlined above upon the overall navigation performance requires knowledge of the receiver architecture and the status of the satellite constellation.

A detailed analysis of these aspects is outside the scope of this report, but the data would appear to support the results and conclusions from the previous availability study reported in [2] (similar estimates for the "Realism Factor" were derived in each case). The overall conclusions from that study were as follows:

> "Exclusive reliance on GPS for helicopter navigation is unsafe."
>
> "Predictive RAIM for helicopter operations will give optimistic results."
>
> "Operational procedures have the potential to compensate for some of the lack of safety, but only if those procedures fully take into account the nature of the weaknesses of GPS for this application."

These statements were based upon flight trials conducted using the same receiver design and tail antenna location as were employed for the present rotor 'interference' experiment. However, in view of the fact that an alternative antenna location on the same aircraft did not appear to exhibit the same problem with availability, it is contended that there is insufficient data to determine how these conclusions may apply to different operational GPS installations. The generality of these statements has therefore not yet been established. Section 8.4 contains some suggestions as to how additional evidence could be gathered to explore the extent to which different aircraft installations are affected by this problem.

8.3 Receiver signal level estimates

From the previous results reported in [1] it had been assumed that the signal level (CNR) figures generated by a GPS receiver would provide a suitable method by which to investigate the impact of the rotor 'interference' and, in particular, to examine how it was observed to vary with such factors as the rotor speed, the rotor blade blockage time, and the antenna position relative to the rotors.

However, following an analysis of the data from the trial it was concluded that these signal level parameters were of limited value due to the fact that the results were not consistent between the three different receivers (for the previous study, data had only been available from the Navstar unit). Appendix A of this report presents a summary of the relevant results and demonstrates that, whereas the Navstar receiver exhibited a progressive degradation in the reported signal level as the rotor speed was increased, the corresponding values computed by the Trimble and ISN receivers remained largely unchanged. In contrast, all three receivers reported a reduction in signal level during tests where the blades were turned slowly by hand. With the rotors running, several instances occurred where a receiver was observed to have lost lock on a satellite (for reasons attributed to rotor 'interference') without there having been any significant reduction in the reported signal level, suggesting that this latter parameter does not necessarily provide a reliable indication for the existence of a tracking problem.

Appendix A also includes the results obtained by applying two alternative 'textbook' CNR estimation techniques to recorded snapshot data from the ISN receiver. The analysis demonstrates that, although the two techniques produce similar estimates in response to an unmodulated (rotors stationary) input, differing results are obtained when the algorithms are presented with data recorded whilst the rotors are running. It is therefore likely that, since no universal method for computing the CNR exists, the various GPS manufacturers have implemented proprietary techniques which provide different results in response to a rotor-modulated input signal. Considerable caution is therefore required when interpreting apparently compatible results from different manufacturers' equipment.

8.4 Airworthiness implications

The results in this report indicate the potential impact of rotor 'interference' upon the performance of a GPS receiver installed in a helicopter, in particular the fact that a significant reduction in the availability of the range measurements was observed with the antenna at one particular location. However, it was also demonstrated that the results obtained with the antenna in a second position were much more benign, even though rotor 'interference' was clearly present in both cases.

In this study it was not possible to examine the impact of all of the variables which could have an influence upon the extent of the rotor 'interference' phenomenon. These might include the following:

blade shape and construction;

antenna position;

shape and construction of the helicopter fuselage;

separation between antenna and rotor disc;

rotor speed;

receiver design.

It must also be recognised that the GPS installation employed for the tests was not totally representative of an operational system since it comprised three different receivers operating from a single antenna via a signal splitter. The trial results therefore only serve to indicate that a potential problem exists, rather than as a benchmark against which the performance of other installations can be compared.

A review of the applicable airworthiness publications reveals that very little in the way of guidance material is available relating to the siting of GPS antennas on helicopters. For example, in [5] it is stated in paragraph 8c(1)(ii)(G):

> "Evaluation of the antenna installation. It is important that the antenna be one that is approved for the particular type of GPS equipment installed. A critical aspect of any GPS installation is the installation of the antenna. Adequate isolation must be provided between the GPS antenna and any other transmitting antenna(s) installed on the aircraft. Shadowing by aircraft structure can adversely affect the operation of the GPS equipment. Typically, a GPS antenna is located forward of the wings on the top of the fuselage to minimize effects of the wings, tail, etc. during aircraft maneuvring. For installations on helicopters, the effects of the rotor blades on antenna performance must be considered."

Although the fact that the rotor blades can affect the 'antenna performance' (and thus by implication the performance of the complete GPS installation) has been recognised in the final sentence, no guidance is provided as to how a candidate antenna position might be evaluated in practice.

In view of the fact that the mechanisms associated with the rotor 'interference' effects are not fully understood and are, in any event, likely to vary between receivers, the most appropriate method for any such evaluation would seem to be based upon performing empirical measurements using a representative equipment installation (GPS receiver, antenna, RF cable, etc) on the helicopter type in question. It is felt that any alternative techniques, perhaps based upon simulating the rotor effects in some synthetic manner, are unlikely to provide satisfactory results.

If it is assumed that any rotor 'interference' problems are likely to manifest themselves as a reduction in range measurement availability, then the goal of an empirical aircraft test should be to investigate whether there is any significant variation in the receiver tracking performance with the rotors running for satellite signals originating from a representative sample of different positions relative to the aircraft. In contemplating such an activity it would be necessary to consider the following:

a) whether the necessary tracking data is available in real time from the GPS receiver: dependent upon the type of installation, it may not always be possible to monitor which satellites are being successfully tracked;

b) whether there would be any benefit in also monitoring the receiver's satellite signal level estimates (the results in Appendix A suggest that considerable caution is required in interpreting these values without knowledge of how they are computed within the receiver);

c) whether it is feasible to undertake the trial in a sufficiently controlled environment to provide meaningful results.

Before making any changes to the arrangements for the approval of GPS equipment and/or operational procedures using GPS, it would seem appropriate to assess the extent of any rotor 'interference' problem on existing operational helicopter GPS installations. One possible option might be to undertake this by means of a limited in-

service measurement trial, perhaps involving a small number of different aircraft types on a sample basis.

Helicopters involved in the CAA's HOMP programme are already configured with data recording equipment and it is conceivable that these could be modified to acquire the necessary data relating to the GPS receivers' tracking performance. Unfortunately no common standard exists among receiver manufacturers for the transmission of satellite tracking data, and so the interfacing issues associated with arranging a trial of this nature would need to be carefully investigated (it is likely that each different model of receiver would need to be considered separately) to confirm whether the necessary parameters can be readily monitored on the various aircraft involved.

9 Summary of Conclusions and Recommendations

9.1 Conclusions

1) The helicopter rotors were demonstrated to introduce a periodic modulation onto the C/A code GPS satellite signals.

2) Rotor 'interference' was identified with the GPS antenna mounted in two different positions (adjacent to the tail rotor and underneath the main rotor) on a Sikorsky S76C helicopter. The nature of the modulation was observed to differ in the two cases.

3) The effect of the rotor modulation upon the carrier-to-noise ratio of the received signals was estimated to be between -3dB and -8dB.

4) No evidence was obtained for the rotor 'interference' having affected the range measurement accuracy of a GPS receiver.

5) Rotor 'interference' was observed to result in a reduction in the range measurement availability with the GPS antenna mounted adjacent to the tail rotor. However it must not be assumed that identical results would necessarily be obtained from other GPS antenna installations adjacent to helicopter tail rotors.

6) Rotor 'interference' was not observed to result in any significant reduction in the range measurement availability with the GPS antenna mounted beneath the main rotor. However it must not be assumed that identical results would necessarily be obtained from other GPS antenna installations beneath helicopter main rotors.

7) A reduction in range measurement availability has the potential to cause a reduction in the overall availability of the navigation function and thus to affect the performance of a GPS installation. The precise impact will be dependent upon factors which vary according to the receiver architecture, the number of healthy satellites visible, and the dynamics of the aircraft.

8) Changes within the GPS space segment, such as the loss of healthy satellites from the constellation (currently there are 27 healthy satellites whereas the United States Government [9] is committed to provide a nominal 24 satellite constellation) or a reduction in transmitted signal power (currently the GPS satellites transmit in the region of 5dB excess power [8]), could result in a further reduction in navigation availability when the rotor 'interference' is present.

9) The effect of rotor 'interference' on the computed signal level (carrier-to-noise) estimates was observed to vary between different designs of receiver. Since two alternative 'textbook' carrier-to-noise estimation algorithms also yielded differing results (when processing the same correlator data), it is suspected that this variation in behaviour was due to implementation differences within the receivers; there is no universally accepted method for computing the signal level parameter.

10) Considerable caution must be applied when interpreting signal level figures generated by a GPS receiver in the presence of rotor 'interference'.

9.2 Recommendations

1) It is recommended that consideration be given to implementing monitoring arrangements which ensure that the impact of any space segment changes can be assessed, with particular attention paid to those aspects where the system performance is currently in excess of that specified by the DoD.

2) It is recommended that consideration be given to undertaking a limited in-service monitoring programme on a sample basis to assess the extent of the rotor 'interference' problem on existing helicopter installations.

3) It is recommended that a review be undertaken of existing operational and airworthiness approvals granted for helicopter GPS installations in order to determine the impact of a potential reduction in availability arising from rotor 'interference'.

4) It is recommended that a review be undertaken of the applicable airworthiness material related to the approval of helicopter GPS installations with a view to providing additional guidance on antenna siting issues and the potential for rotor 'interference'.

5) It is recommended that for future receiver equipment standards a standard method of computing CNR is used.

6) It is recommended that for future receiver equipment standards CNR and individual satellite tracking status be provided as standard receiver outputs, in order to support operational evaluation of the equipment.

Appendix A Receiver Signal Level Estimates

1 Introduction

In addition to the availability flags discussed in Section 7, most GPS receivers also provide an indication of the 'tracking quality' for each satellite. This is normally presented in the form of a signal level estimate derived from an analysis of the correlation values for the channel in question.

These signal level measurements are often expressed as an estimate of the Carrier-to-Noise Ratio (CNR), a communications engineering concept which relates the energy contained in the 'desired' signal available to the receiver (a function of transmitter power, antenna gain and propagation losses), to the inevitable 'undesired' energy arising from noise sources. These noise sources are commonly modelled as a wideband signal with a flat power spectral density, and direct comparison with a specified input signal will require knowledge of the applicable bandwidth. CNR is normally expressed in units of dBHz which can be regarded as the absolute signal-to-noise ratio in a 1Hz bandwith.

Some receiver types which do not directly provide an indication of the CNR, instead generate a dimensionless signal level parameter which is often based upon a system of units (either linear or logarithmic) proprietary to the manufacturer. In some receivers this indication can be very simple, for example it has been observed that there are systems which output a single digit in the range 0 to 9 as a representation of the signal quality.

In this Appendix the behaviour of two alternative CNR estimators are assessed using the recorded correlator snapshot data from the ISN receiver. These results are then compared with the 1Hz signal level estimates which were output in real time by the Navstar, Trimble and ISN receivers.

2 Performance of two alternative CNR estimators

The available literature reveals a number of different techniques for the estimation of the CNR from correlation measurements on a receiver channel. For this analysis two different estimators have been employed and will be distinguished by the initials of the two authors. A detailed explanation of the algorithms involved is outside the scope of this report.

The 'AJ estimator' [6] involves the calculation of signal and noise power in two different bandwidths; a narrow band and a wide band. The bandwidths are defined by parameters termed K and M, and for this analysis the values of K and M were set to 50 and 20 respectively; the same values used in [6].

The 'JJ estimator' [7] operates only on 1-bit sampled data and is the technique employed within the ISN receiver to generate its real time CNR estimate based upon a 1s summation of the in-phase (I_p) correlation data.

Figure 1 presents the performances of these two CNR estimators for the snapshot data shown previously for PRN 28 whilst the rotors were stationary, obtained using the tail antenna. It can be seen that the two estimation techniques are in good agreement for the 10s of data captured, agreeing to within 0.5 dBHz.

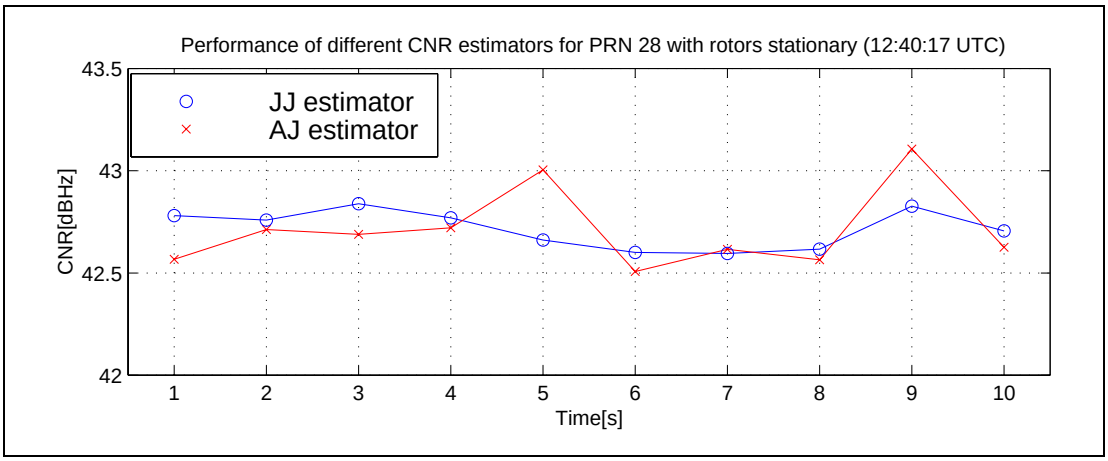

Figure 1 Comparison of CNR estimators for PRN 28 data - rotors stationary

The performance of the two estimators when presented with data from a subsequent period during which the rotors were turning is shown in Figure 2. This data is again for PRN 28, with the rotors turning at a recorded speed of 62.5% Nr. For this data set there is a large discrepancy between the CNRs calculated by the two estimators. The results from the AJ estimator are between 4.2 and 4.7 dBHz lower than those from the JJ estimator, the mean difference being 4.5 dBHz. In addition the JJ estimator's CNR values are clearly very similar to those shown previously in Figure 1, which was based on a recording taken less than three minutes earlier. This suggests that the received signal level had not varied much during this time, and also that the oscillations in the correlation data due to the tail rotor motion have not had a significant impact upon the CNR derived from the JJ estimator.

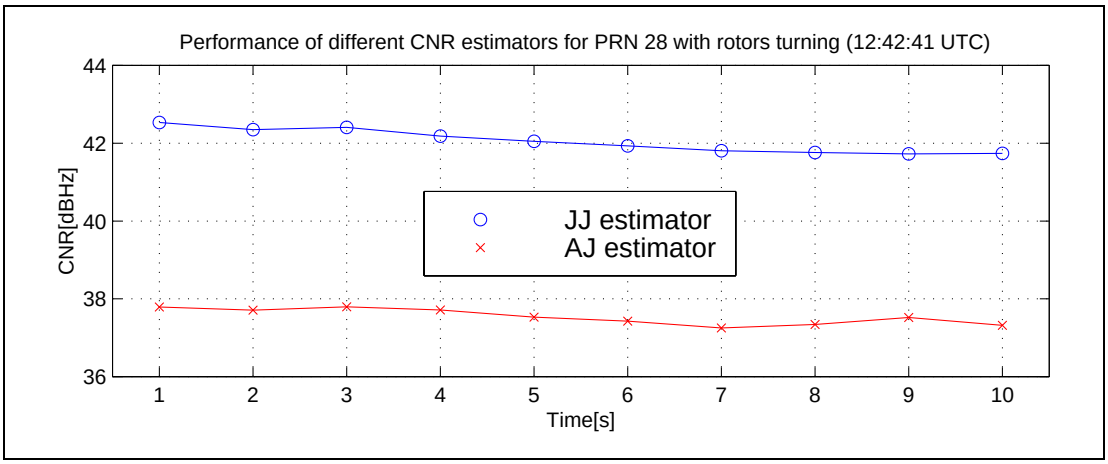

Figure 2 Comparison of CNR estimators for PRN 28 data - rotors turning

Figure 3 presents the estimated CNR values for snapshot data gathered for PRN 30, again using the tail antenna, during a period when the rotors were stationary. The two estimators are once again in reasonably good agreement, with the AJ estimator derived values being between 0.6 and 1.5 dBHz below those obtained using the JJ estimator.

This can be compared with Figure 4 which depicts the performance of the two estimators using the PRN 30 snapshot data when the rotors were turning at 74.5% Nr. Once again there is a large discrepancy between the two sets of results , with the estimate derived using the AJ technique being an average of 4.0 dBHz lower than that using the JJ technique.

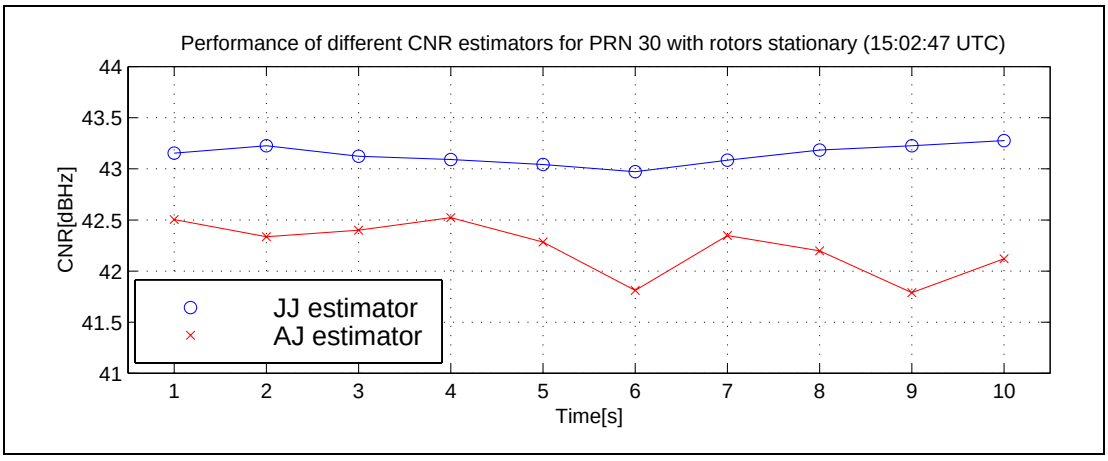

Figure 3 Comparison of CNR estimators for PRN 30 data - rotors stationary

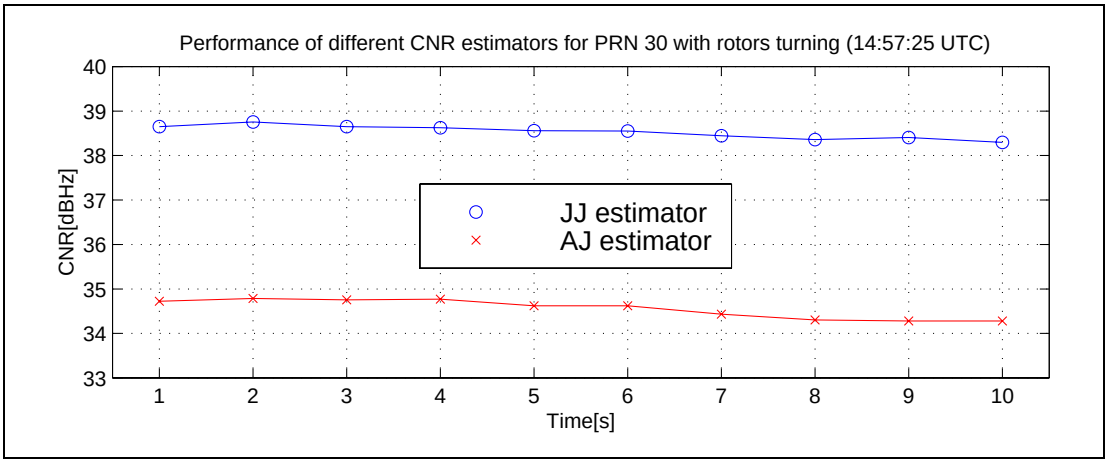

Figure 4 Comparison of CNR estimators for PRN 30 data - rotors turning

In order to further investigate the difference between the results from the JJ and AJ estimator techniques in the presence of rotor 'interference', an analysis was performed based upon a larger number of snapshot data sets with the rotors running at full speed. The results, based upon data for both PRN 28 and PRN 30, are shown in Figure 5 and reveal that the AJ technique produced CNR estimates which were between 2.5 and 5.0 dBHz lower than those using the JJ technique.

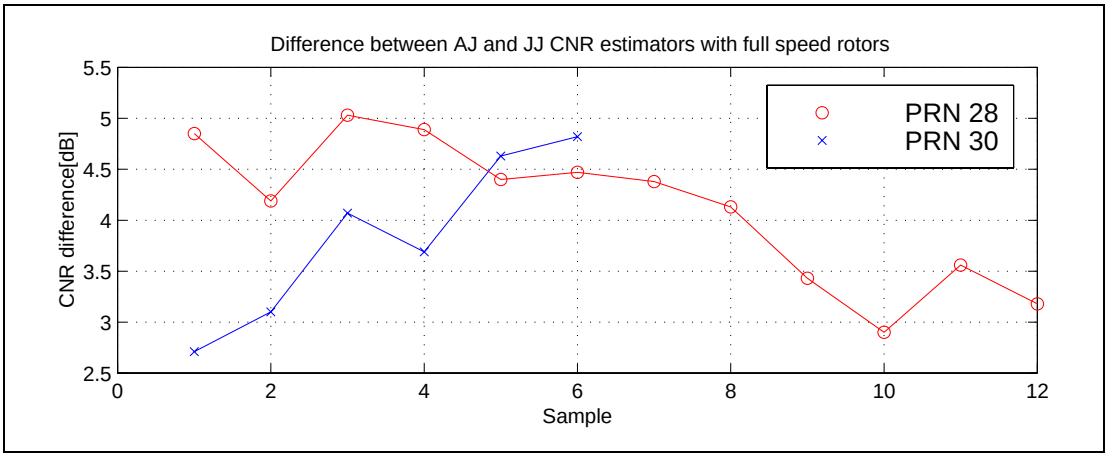

Figure 5 Differences between two different CNR estimators - rotors at full speed

3 Real time signal level estimates - tail rotor

Of the three GPS receivers employed for the rotor experiment, both the Navstar and the ISN units generated real time CNR estimates in units of dBHz. The corresponding output from the Trimble receiver was in the form of a dimensionless 'Signal Level' value.

With the receivers connected to the tail mounted antenna, Figure 6 shows how the reported signal level estimates from the three receivers varied as the rotors were turned slowly by hand through about 1.5 rotations (six blade passages) at the tail rotor, for two satellites (PRN 7 and PRN 28) where the signal path intersected the tail rotor disc. A transient reduction in signal level associated with passage of the blades can be observed for all three receivers, the reduction being of the order of 5 to 9 dBHz for the Navstar and ISN data and 5 to 7 signal units for the Trimble data. The ISN receiver lost lock on PRN 28 at the first blade passage and tracking was not regained before the end of the recording. A transient loss of lock, lasting for only 1s, also occurred on this satellite with the Trimble receiver at time 13:52:08.

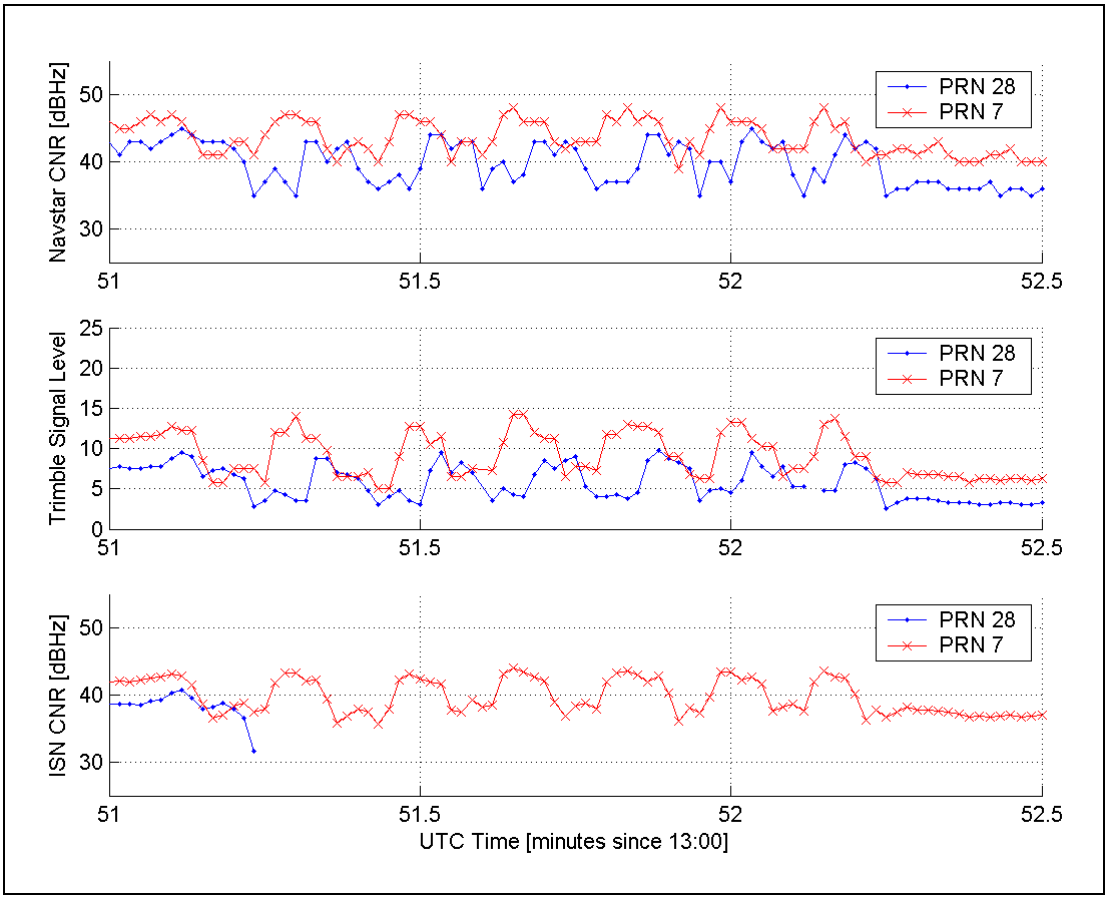

Figure 6 Signal level variation during manual rotation - tail rotor

The results obtained via manual rotation of the blades can be contrasted with those shown in Figure 7, which depicts the signal level variation over the course of a complete rotor start/stop sequence for three satellites where the signal path intersected the tail rotor disc. It may be observed that the CNR reported by the Navstar receiver reduced, by around 10 dBHz, during the rotor-running period but that a similar effect was not observed with either the Trimble or ISN data (there is some evidence for a slight reduction as the rotors were started, but no corresponding increase at the end of the period).

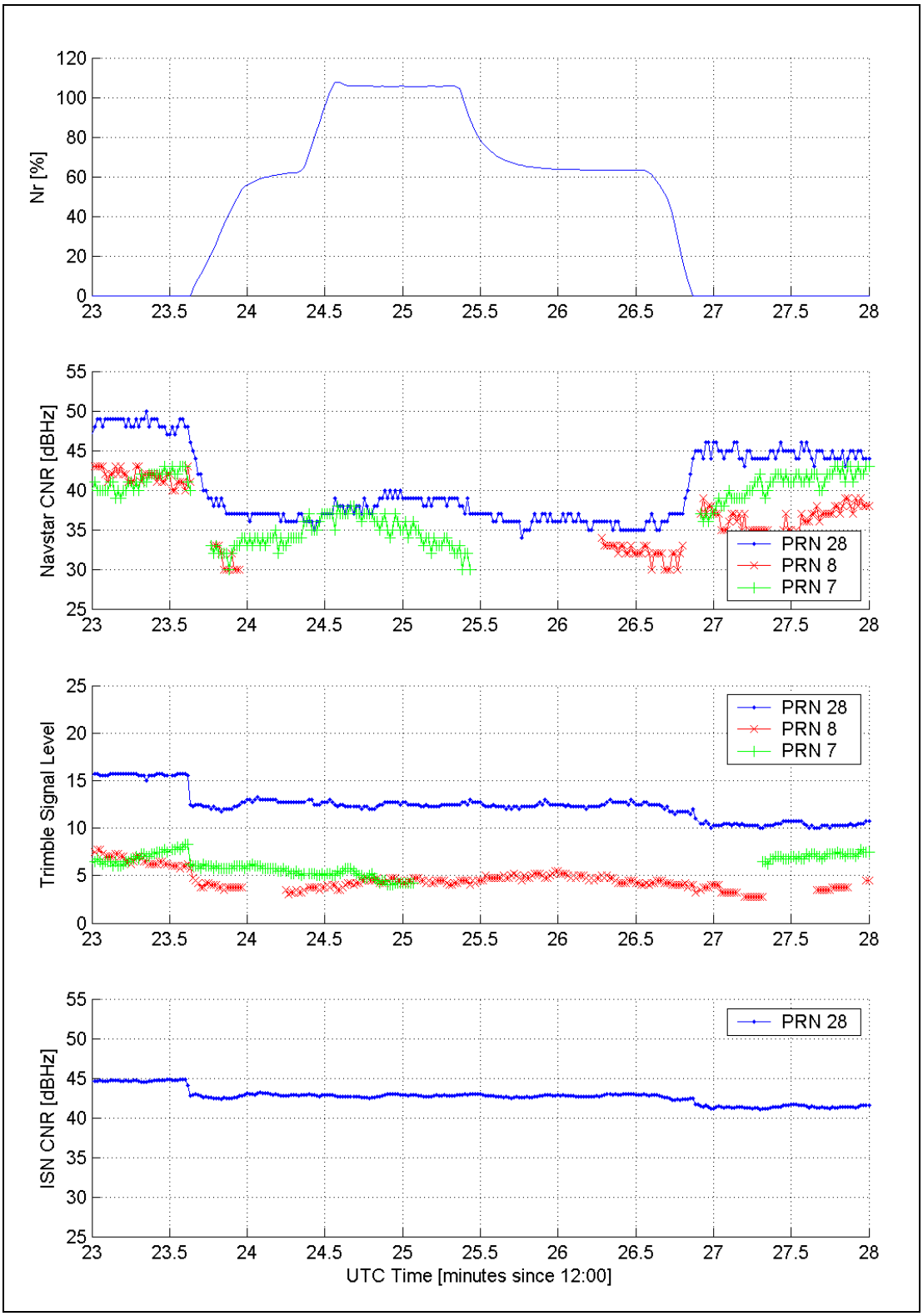

Figure 7 Signal level varation during start/stop sequence - tail rotor

Figure 8 and Figure 9 are 'pierce-point"' diagrams, showing the intersection of the signal paths with the tail rotor disc for the satellites whose signal level data was plotted in Figure 6 and Figure 7 respectively. The diagram can be thought of as the projection of the point of intersection into the plane of the tail rotor disc, viewed from the port side of the helicopter.

For each satellite, the relative azimuth (degrees clockwise from the aircraft nose) and elevation (degrees above the horizon) is also shown, together with the percentage mark:space ratio associated with passage of the rotor blades. The latter varies with distance from the hub owing to the fact that the blade chord remains approximately constant along its length.

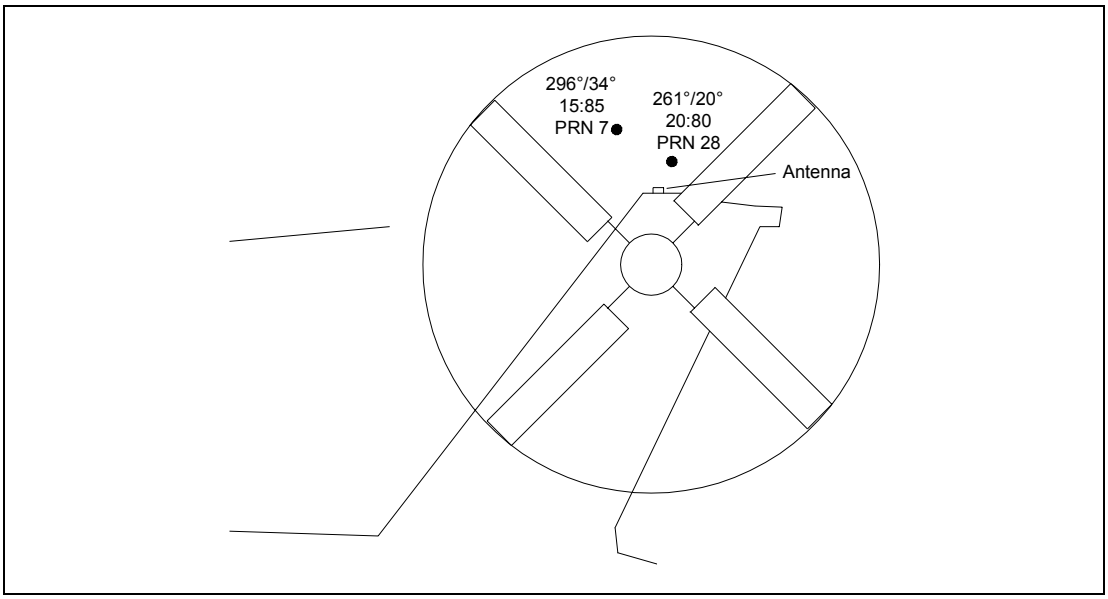

Figure 8 Intersection of signal path with tail rotor disc for satellites in Figure 6

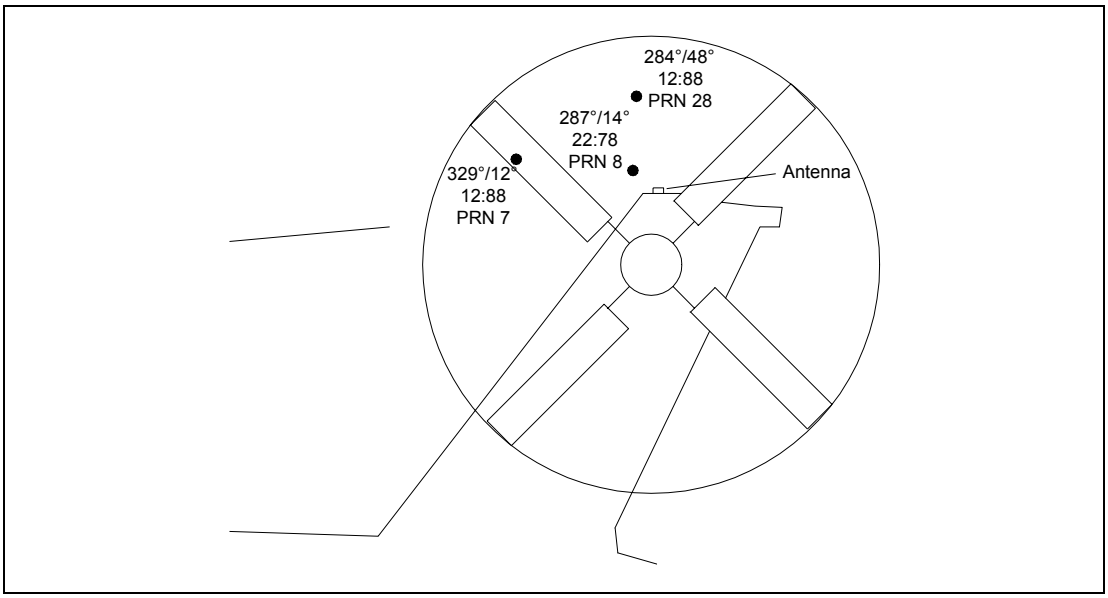

Figure 9 Intersection of signal path with tail rotor disc for satellites in Figure 7

Analysis of similar data for the other start/stop sequences using the tail antenna reveals broadly consistent results, with the Navstar receiver's CNR estimates being degraded whenever the rotors were running: the effect was slightly worse at ground idle (maximum reduction 7 to 11 dBHz) than at full speed (maximum reduction 5 to 8 dBHz). A slightly lesser degradation was observed with satellite signals which did not intersect the rotor disc.

This can be contrasted with the behaviour of the other two receivers' signal level estimates, where the effect of running the rotors appeared to be variable with changes (in both directions) observed of up to 5 units for the Trimble receiver, and 1 to 2 dBHz for the ISN receiver. The greatest changes appeared to consist of transient events associated with the instants when the rotors began to turn or as they came to rest.

This difference in behaviour is immediately apparent from Figure 10 where the PRN 28 signal level estimates from the three receivers have been plotted against rotor speed for two consecutive start/stop tests. The progressive increase in degradation of the reported Navstar CNR between zero speed and 30-40% Nr is readily apparent, whereas the signal level values reported by the Trimble and ISN systems do not vary significantly at different values of Nr.

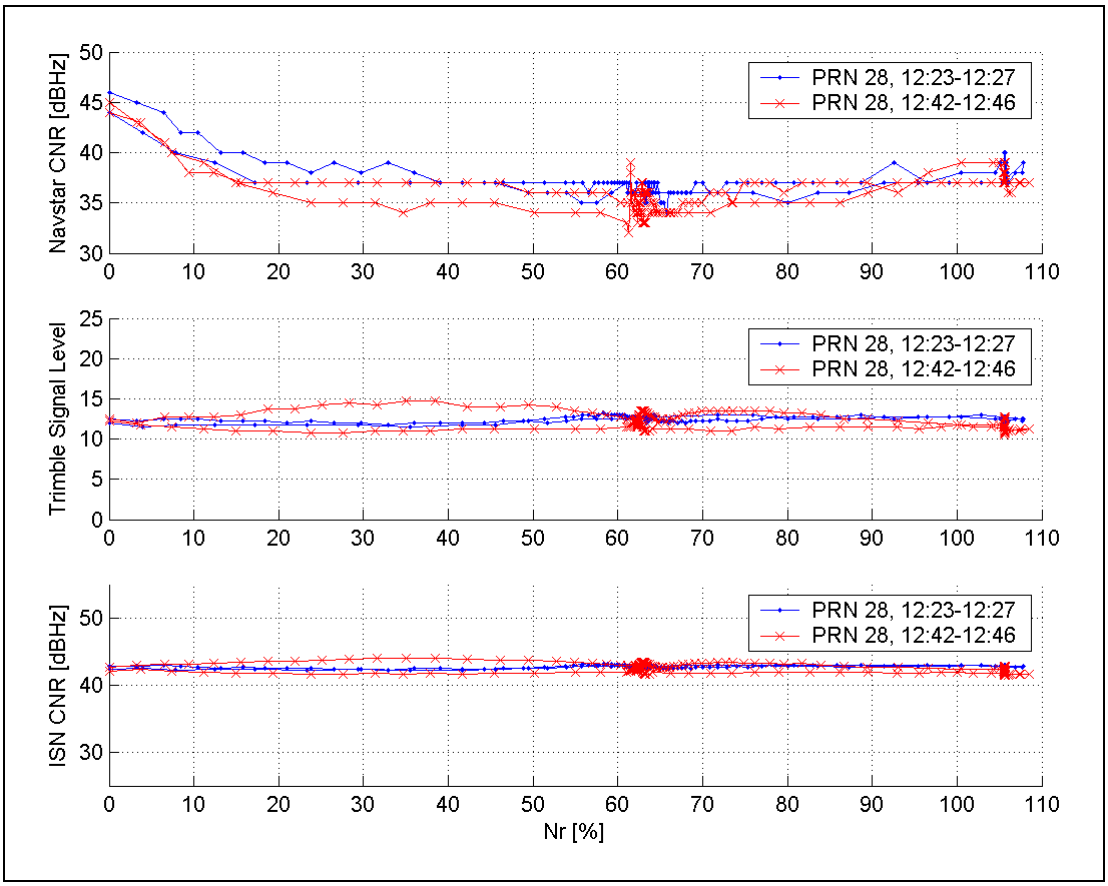

Figure 10 Signal level variation with rotor speed - tail rotor

4 Real time signal level estimates - main rotor

Figure 11 presents the results obtained during manual rotation of the main rotor through 90° anticlockwise and then back to its original position. This caused one main rotor blade to pass twice between the nose mounted antenna and the two satellites PRN 14 and PRN 30 (the corresponding 'pierce-point' plot, viewed from above the

helicopter, is shown in Figure 12). Transient reductions in the signal level from all three receivers were observed, although the magnitude of the changes was in some cases somewhat less than that observed during the corresponding tail rotor test.

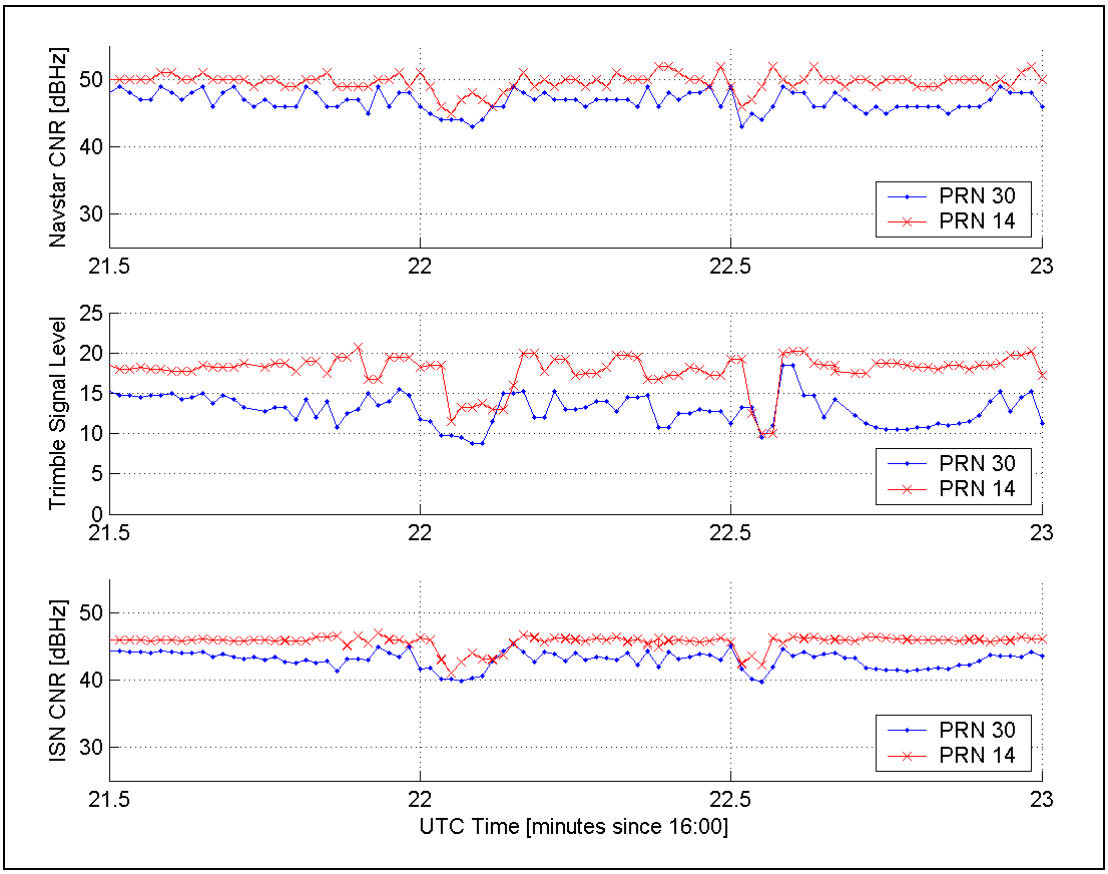

Figure 11 Signal level variation during manual rotation - main rotor

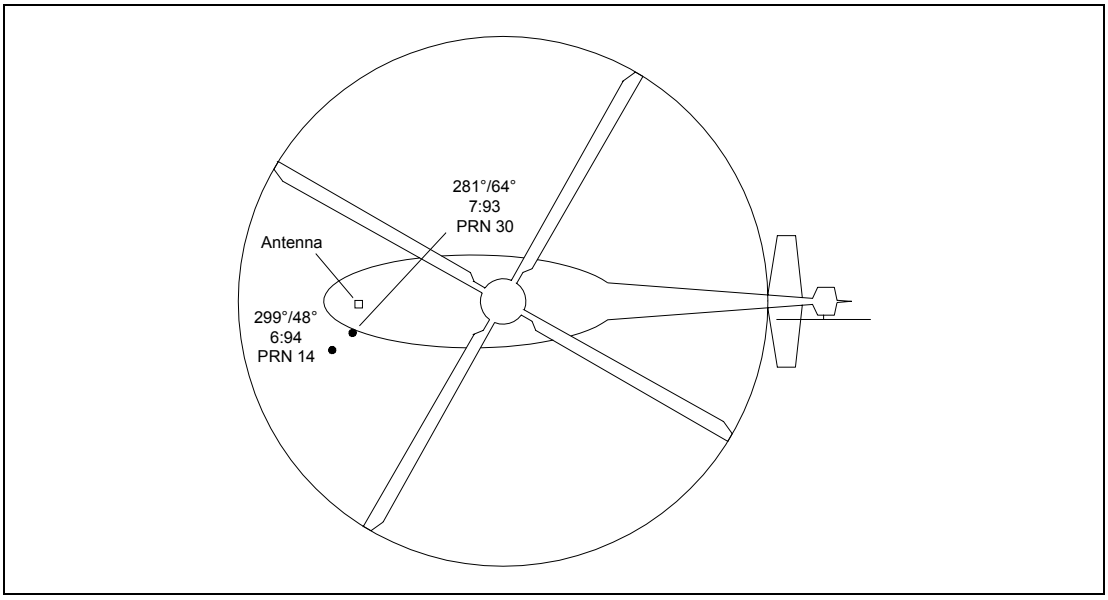

Figure 12 Intersection of signal path with main rotor disc for satellites in Figure 11

The results obtained during a start/stop test with the nose antenna in use are shown in Figure 13, for PRN 14 and PRN 30. Unfortunately only a partial data set was available from the ISN receiver which ceased recording shortly before 15:42 UTC. However, the available results clearly demonstrate that the behaviour of the Navstar signal level estimate again differs from that generated by the other two receivers.

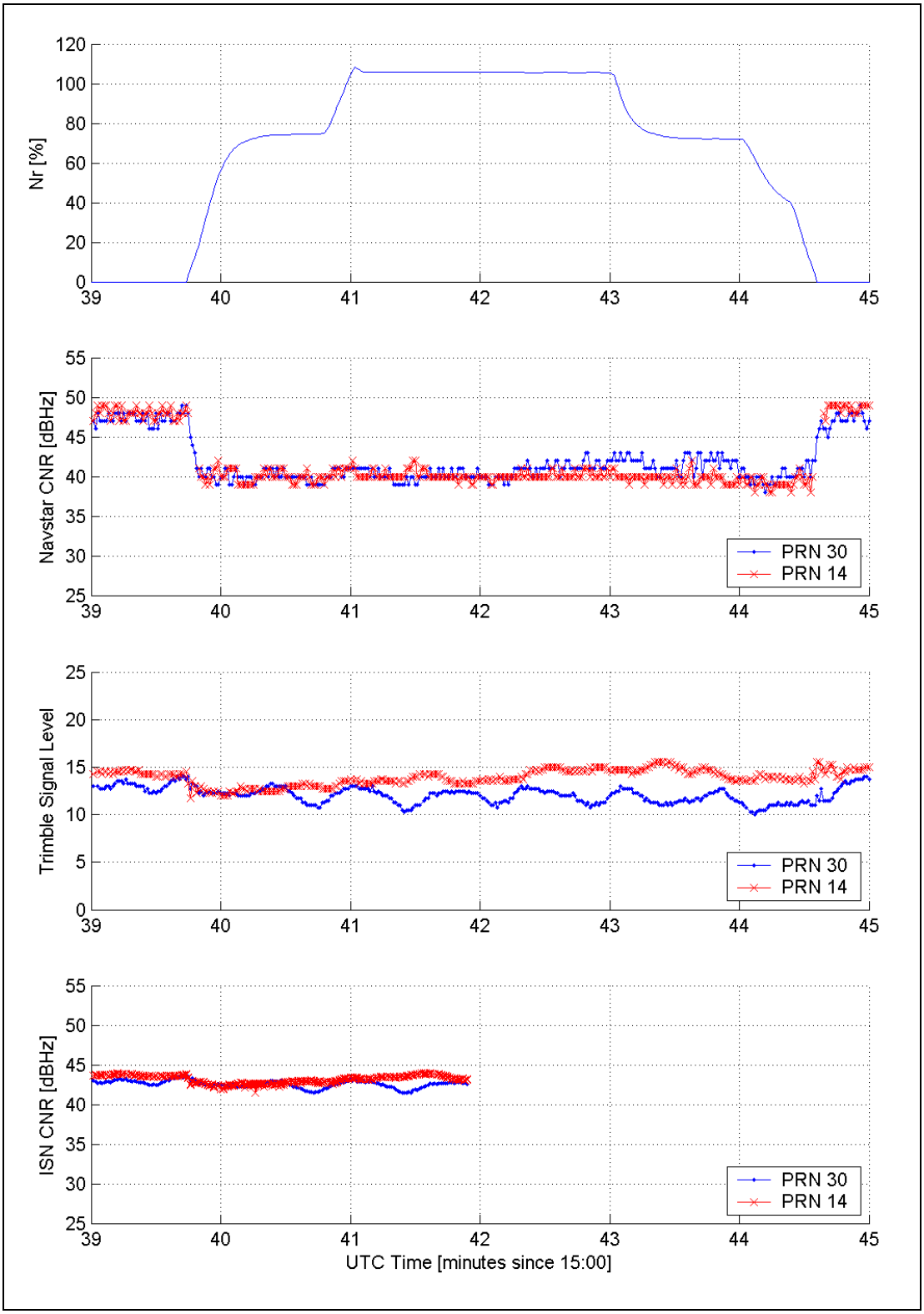

Figure 13 Signal level varation during start/stop sequence - main rotor

Analysis of this test revealed very similar results for another four satellites (PRN 4, PRN 5, PRN 7 and PRN 9) where the signal path also intersected or passed close to the main rotor disc: a 'pierce-point' plot for all six satellites is shown in Figure 14. The Navstar CNR degradation was lowest for PRN 4 and PRN 7 which are at the lowest elevation, and for which the mark:space fraction is the smallest.

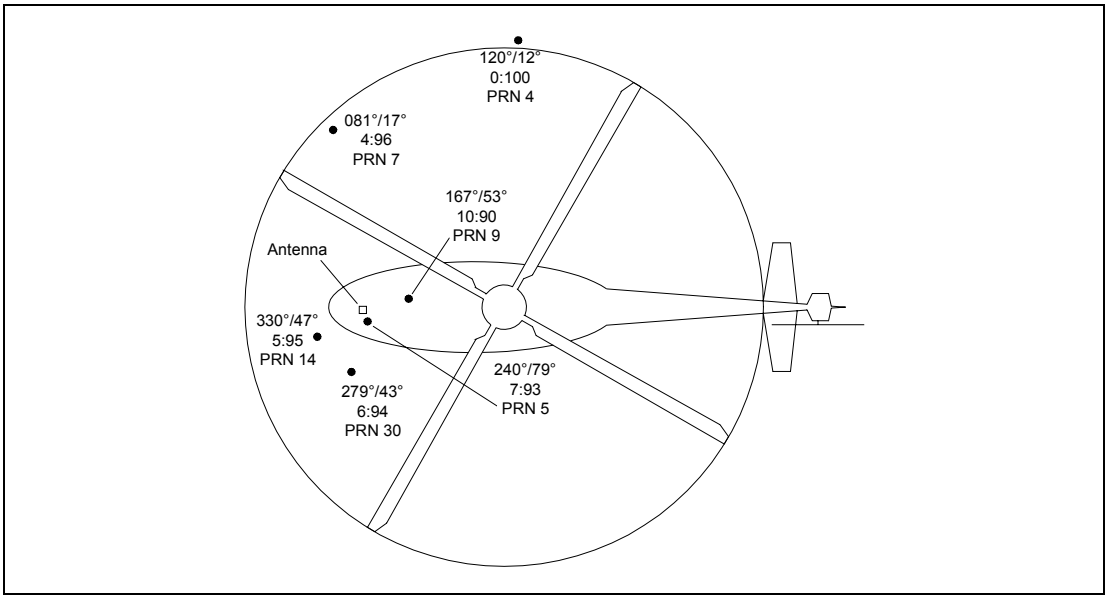

Figure 14 Intersection of signal path with main rotor disc for satellites in Figure 13

5 Summary

These results demonstrate the limitations of relying on the signal level estimates generated by the different receiver designs as an indication for the presence of rotor 'interference'. This is evident from the fact that there was a reduction of several dB in the signal level output by the Navstar receiver correlated with the rotors running period, whereas the same consistency was not observed with the corresponding measurements from the Trimble and ISN receivers. However, a reduction in signal level could be demonstrated to occur with all three receivers through manual positioning of a rotor blade.

When combined with the fact that the greatest transient changes in the Trimble and ISN signal levels occurred when the rotors were turning very slowly, this suggests that the estimation algorithms employed by the latter two receivers may not be capable of detecting the short duration attenuation events associated with rotors turning at higher speeds. Support for the hypothesis that the various manufacturers have implemented incompatible algorithms is provided by the response of the two 'textbook' estimators, which were demonstrated to produce different results when presented with data affected by the rotor modulation, even though their response to rotors stationary data was very similar.